UNCLASSIFIED

Summary Report

Copy # 17

Date: July 1970

DESIGN OF LIQUID AMMONIA BATTERY (U)

J. R. Backlund

AMCMS Code: 5566.12.50908

Honeywell Inc.
Livingston Electronic Laboratory
Route 309
Montgomeryville, Pennsylvania 18936

Contract No.: DA-28-017-AMC-1542(A)

Prepared for:

Department of the Army
Picatinny Arsenal
Dover, New Jersey 07801

UNCLASSIFIED

Honeywell

LIVINGSTON ELECTRONIC LABORATORY

UNCLASSIFIED

Summary Report

Copy # 17

Date: July 1970

DESIGN OF LIQUID AMMONIA BATTERY (U)

J. R. Backlund

AMCMS Code: 5566.12.50908

Honeywell Inc.
Livingston Electronic Laboratory
Route #309
Montgomeryville, Pennsylvania 18936

Contract No.: DA-28-017-AMC-1542(A)

Prepared for:

Department of the Army
Picatinny Arsenal
Dover, New Jersey 07801

UNCLASSIFIED

(a)

TABLE OF CONTENTS

LIST OF FIGURES AND ILLUSTRATIONS

ABSTRACT (U)

Design of Liquid Ammonia Batteries

This report summarizes work done in the design of a primary reserve liquid ammonia battery capable of satisfying the particular requirements of one application which include 24-volt multitap output delivering eight voltage levels at various currents for a period of 50 hours at -65°F to +160°F.

Efforts consisted principally of packaging of existing liquid ammonia chemistry in an advanced mechanical configuration. Major innovations in design were yielded in the form of activation mechanics and the minimization of intercell electrical leakage. All technical specifications were met by the resultant design except for voltage regulation at each output tap for the entire discharge period.

Summary (U)

The work described herein was accomplished by Honeywell Inc., Livingston Electronic Laboratory, under Contract No. DA-28-017-AMC-1542(A) for the application of liquid ammonia chemistry to one specific battery requirement.

Efforts have been applied over a four-year period to design a primary reserve battery to meet specific performance and environment requirements using liquid ammonia chemistry to advance the general capability of batteries presently in existence. General objectives of this design include a 24-volt multitap output delivering various currents at +2, +4, +6, +12 and -2, -4, -6, -12 taps over a period of 50 hours at all temperatures between -65°F and +160°F. Additional pulses of energy are required at 24 volts after the 50-hour discharge.

Application of liquid ammonia chemistry systems to this requirement has necessitated major innovations in packaging technology, and it is considered to be the most complex liquid ammonia design evolved to date. Two problems overcome in the course of this contract include rapid reserve transport of larger quantities of liquid ammonia than ever attempted before (~400 cc) and protection of the nine closely spaced terminal pins within a highly corrosive electrolyte atmosphere.

Complete satisfaction of all the program's objectives were not entirely achieved. Investigations performed on the various electrochemical systems compatible with liquid ammonia indicated certain inherent characteristics within each system prevented total achievement in meeting the minimum voltage requirement after a 50-hour discharge. In all other respects the program results reflect a substantial advancement in application techniques for use in liquid ammonia electrochemical devices.

1.0 Introduction (U)

(U) 1.1 Over a period of four years, efforts have been applied to design and package a primary reserve battery using liquid ammonia electrochemistry to meet the environmental and performance requirements of this program. These efforts were applied towards increasing the ability of existing electrochemical systems in order to meet this goal.

(U) 1.2 To improve the performance of the organic system over the temperature range, a variety of materials were selected on the basis of their previous performance and reviewed to meet this goal. These materials included several organic cathodes, the use of standard and expanded light metals for the anode, and different types of separator material.

(U) 1.3 The complexity of the multi-terminal design necessitated a major improvement in the insulation material and the method of isolating this area from the corrosive atmosphere of the electrolyte. A large number of new materials and techniques were investigated in an attempt to prevent intercell electrical leakage, which was considered to be a major deterrent to satisfactory battery performance.

(U) 1.4 New concepts in battery packaging were realized because of the large volume of electrolyte required for operation and the restrictive packaging limits imposed by the design requirement. Improvement incorporated into the design of the hardware include a safety vent which limits operating pressure in the event of internal short circuits, a redesigned activation diaphragm which increases the reliability of the unit, generally improved case construction details, modifications to the gas generator activation portions of the battery, and the package treatment necessary to accommodate multiple voltage taps.

2.0 Description of Battery and Specifications (U)

(U) 2.1 The XM-19 Emplacement Site Battery is a liquid ammonia primary reserve power source with nominal dimensions of eight inches in length and four inches in diameter. This fully self-contained unit is to be housed in a stainless steel case with a grenade-type pull ring at one end for initiating the process of primer activation. On the opposite or terminal plate end of the battery there is a multipin connector, at which various output voltages are available, and a safety pressure relief valve.

(U) 2.2 Desired electrical performance is as follows:

Voltage: 24 volts nominally tapped at ±2 v, ±4 v, ±6 v, ±12 v, and 0 v.

Voltage Regulation Ranges:

Voltage Tap	Maximum Voltage	Minimum Voltage
+12	+13.32	+10.68
+ 6	+ 6.66	+ 5.34
+ 4	+ 4.44	+ 3.56
+ 2	+ 2.22	+ 1.78
- 2	- 2.22	- 1.78
- 4	- 4.44	- 3.56
- 6	- 6.66	- 5.34
-12	-13.32	-10.68
0	0	0

Activation Time: Three seconds

Temperature Range: -65°F to +160°F

Current Requirements: During the first 50 hours following activation, the battery shall remain within the listed voltage regulation ranges when operated on standby loads shown on the Schematic of Voltages and Loads presented as Figure A. Ten periods of full scale operation as also shown on the Schematic occur periodically during the same 50-hour period with each full scale operating period lasting five seconds.

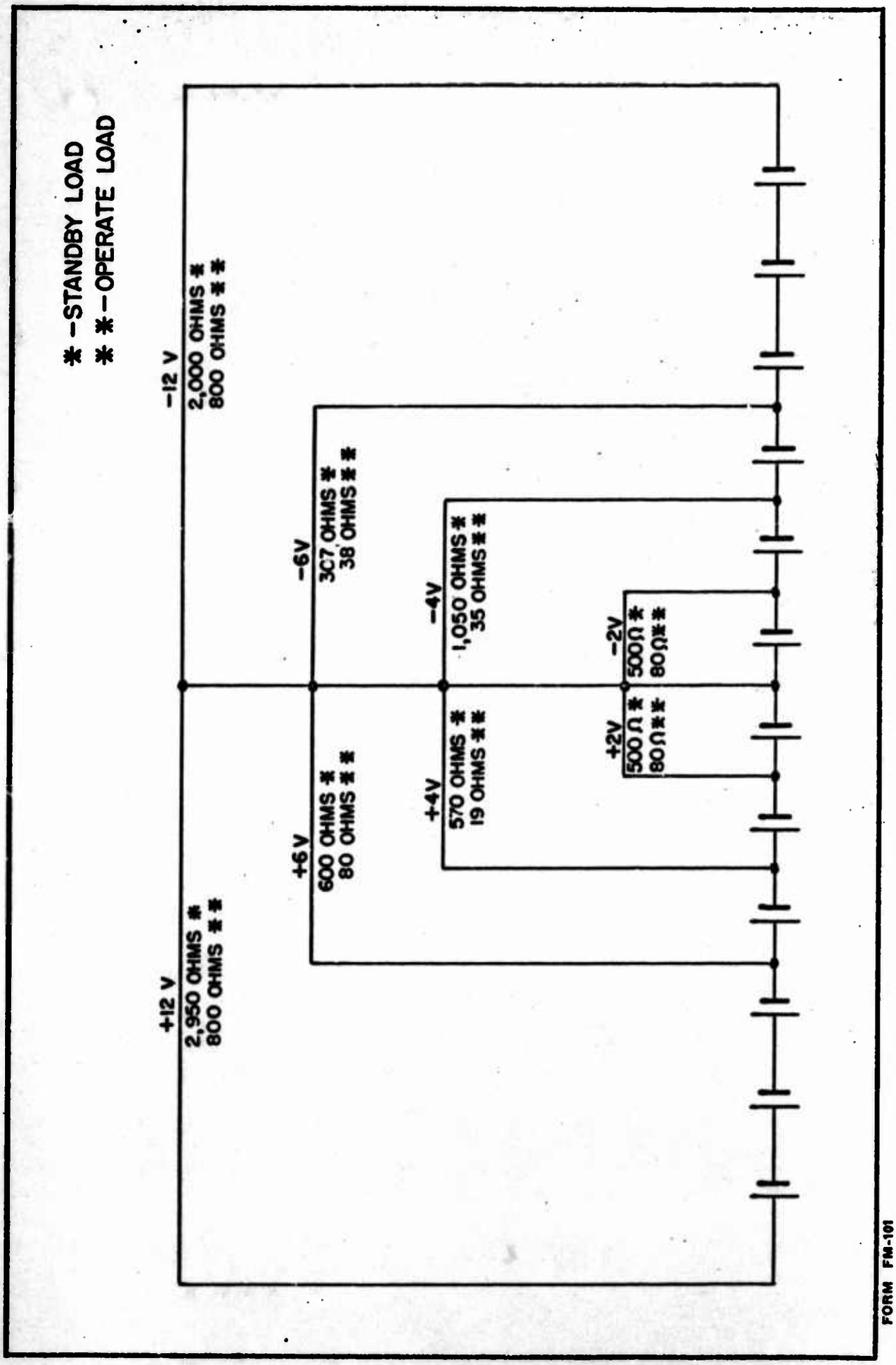

Figure A

Battery Output Schematic

3.0 Summary of Key Technical Activities in Chronological Order (U)

(U) 3.1 A basic working cell structure was established, including the determination of practical cell geometries. These single cells, appropriate for discharge in test chambers, were used to obtain characteristic performance data which might be representative of battery parameters such as discharge life, voltage regulation, discharge rate, internal impedance, cell capacity, and pulse capability. This information was used as a control basis and a point of departure for exploration of high discharge rates and long life capabilities in terms of this particular requirement.

3.1.1 A spiral wound cell configuration was evaluated and found to be physically acceptable in terms of energy density (calculated) and the form factor goals of the requirement.

3.1.2 A flat plate cell configuration of the sandwich-type construction was also found to be an appropriate candidate geometry.

(U) 3.2 A test regime allowing for "worst case" testing was established. "Worst case" testing is in this instance the execution of pulse loads late in the discharge life, since that is the most strenuous condition under which battery cells must operate.

3.2.1 Cells were tested at three environmental levels: -65°F, room ambient (approximately +75°F), and +160°F.

(U) 3.3 Alternate cell variations were tested on a comparative basis in order to overcome performance deficiencies as observed on a single cell basis. These variations included changes in chemical discharge requirements by using

breadboard models of electronic modules as test loads. This was done because of the unique counter-type pulsing load required by the end device.

(U) 3.6 Complete prototype batteries were tested over the environmental test range. Analysis of results and extensive postmortem activities were applied to ascertain failure modes and design weakness. As identification was made of detrimental or design aspects, and corrective measures were added for subsequent series of evaluations. Considerable redesign was necessary with respect to cell and activator packaging because of the strenuous nature of packaging requirements and the multiple voltage output requirements.

3.6.1 Cell insulation, packaging, liquid distribution manifolding, and terminal plate seals were among the redesign considerations.

3.6.2 Complete prototypes were tested to verify all design changes.

(U) 3.7 A quantity of units were subjected to military standard temperature cycle testing. Results were acceptable except for an observed deficiency, which made an extended redesign necessary.

3.7.1 The capacity of the battery unit was discovered to be sufficient to cause rupture of the case when internal short circuit was developed. This internal shorting was caused by breakdown of cell structure from high activation injection damage. When cell energy was released in the form of heat rather than output current, resultant high pressures exceeded case seal limitations.

3.7.2 Extensive redesign measures were executed in order to obtain a more desirable level of reliability with respect to previously observed deficiencies.

3.7.2.1 Activation pressures were rescheduled to minimize liquid injection damage to cell insulation.

3.7.2.2 A "frost plug" vent device was installed to eliminate possible hazards involved with respect to safety.

3.7.2.3 Cell stack structures were reinforced and redimensioned to allow less liquid injection damage.

3.7.2.4 Theoretical studies were made of liquid transport pressure relationships by both the contractor and contracting agency. High speed x-ray pictures were used to investigate the nature and causes of injection damage to cell stacks.

(U) 3.8 Prototype batteries of essentially a second generation design were fabricated and tested, with results showing the fortification measures to be effective. Electrical performance was, however, only marginally satisfactory at temperature extremes.

3.8.1 Along with redesign measures, a modification in form factor was requested, offsetting the multitap connector to one side to facilitate interface with the battery housing of the weapon device. A revised load requirement was effected, redistributing output rates less equitably across certain of the voltage taps.

(U) 3.9 Studies were made of battery heating effects with respect to potential interference with other system components. Tests of units in system hardware showed these effects to be less severe than expected, and also showed some degree of correlation to battery output.

(U) 3.10 End test and evaluations were conducted with success in all performance parameters except for voltage regulation under pulse loads at end of life. Final testing was done using complete batteries mounted in end-item weapon housings.

4.0 Cell and Stack Design (U)

(U) 4.1 During the initial phase of the program, a review of previous developmental efforts using an existing liquid ammonia nonaqueous electrochemical system indicated the capability of satisfying, at the single cell level, the requirements of the program. Single cell tests were conducted using organic cathodes and light metal alloys for the anode for the purpose of accumulating reliable performance data for reference during the later phases of multicell development. The performance characteristics of the cells were studied over the temperature range in order to evaluate and select an optimum electrochemical composition and cell design.

4.1.1 Cell parameters of critical concern were investigated using a planned introduction of variables in fractional factorial patterns. Topics under investigation included optimized cathode content, surface reaction area per cell, optimum electrolyte concentration, cathode solubility, separator thickness, and cell geometry.

4.1.2 Cell output uniformity, as well as operational characteristics such as voltage drop under pulse loads, was compared. Although performance established was relatively uniform throughout the temperature range, the cold temperatu (-50°C) performance was judged to be the design center performance level. Figure B shows results obtained in two different single cell packages, each meeting minimum specified discharge life.

(U) 4.2 Initial tests and experiments were conducted with single flat plate cells in quick coupler test assemblies, as shown in Figure C. These tests were followed by testing of the wrap-type single cell illustrated in Figure D. (Figure D also shows an illustration of flat plate construction for the single cell.)

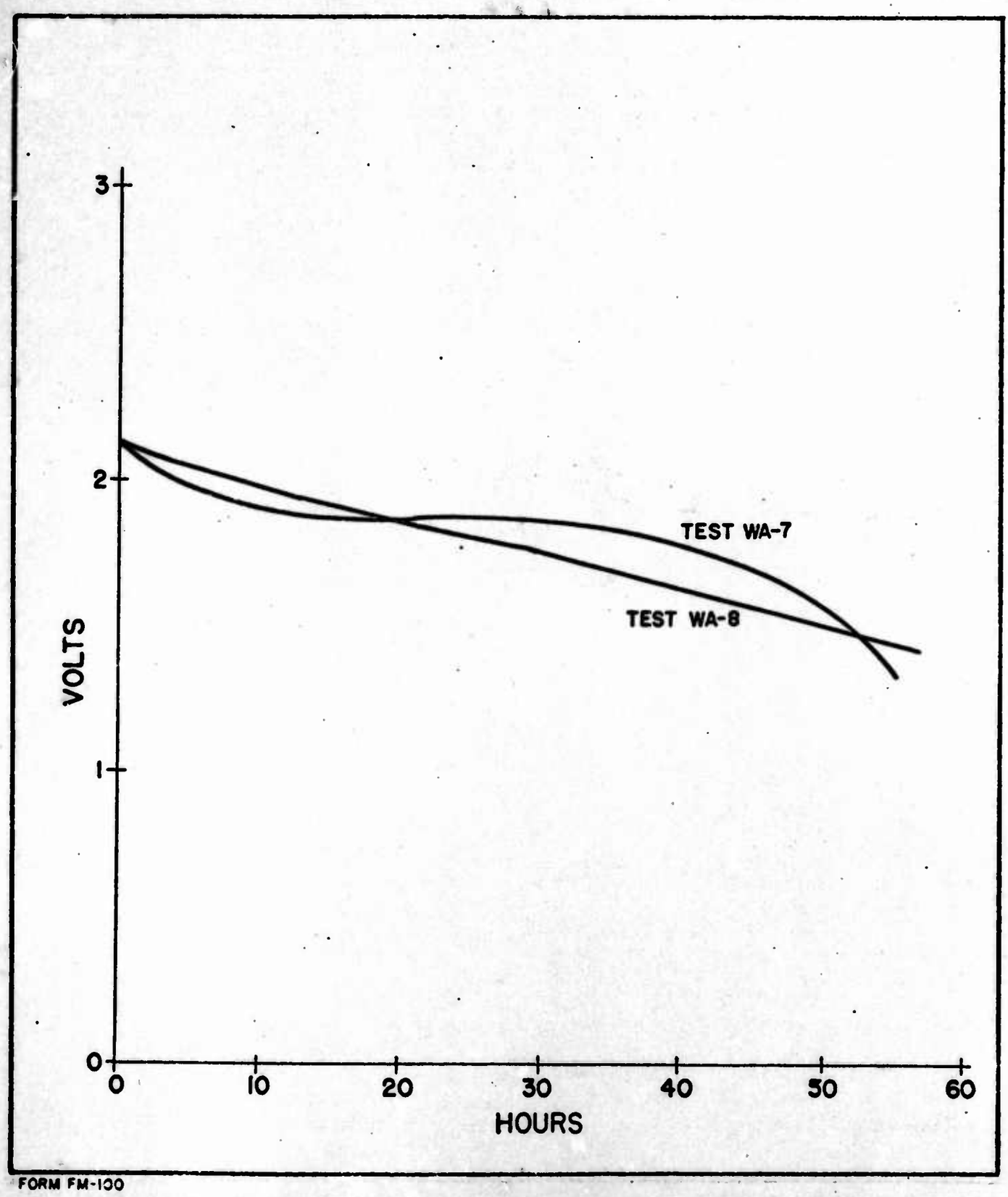

Figure B

"A" Single Cell Performance -50°C

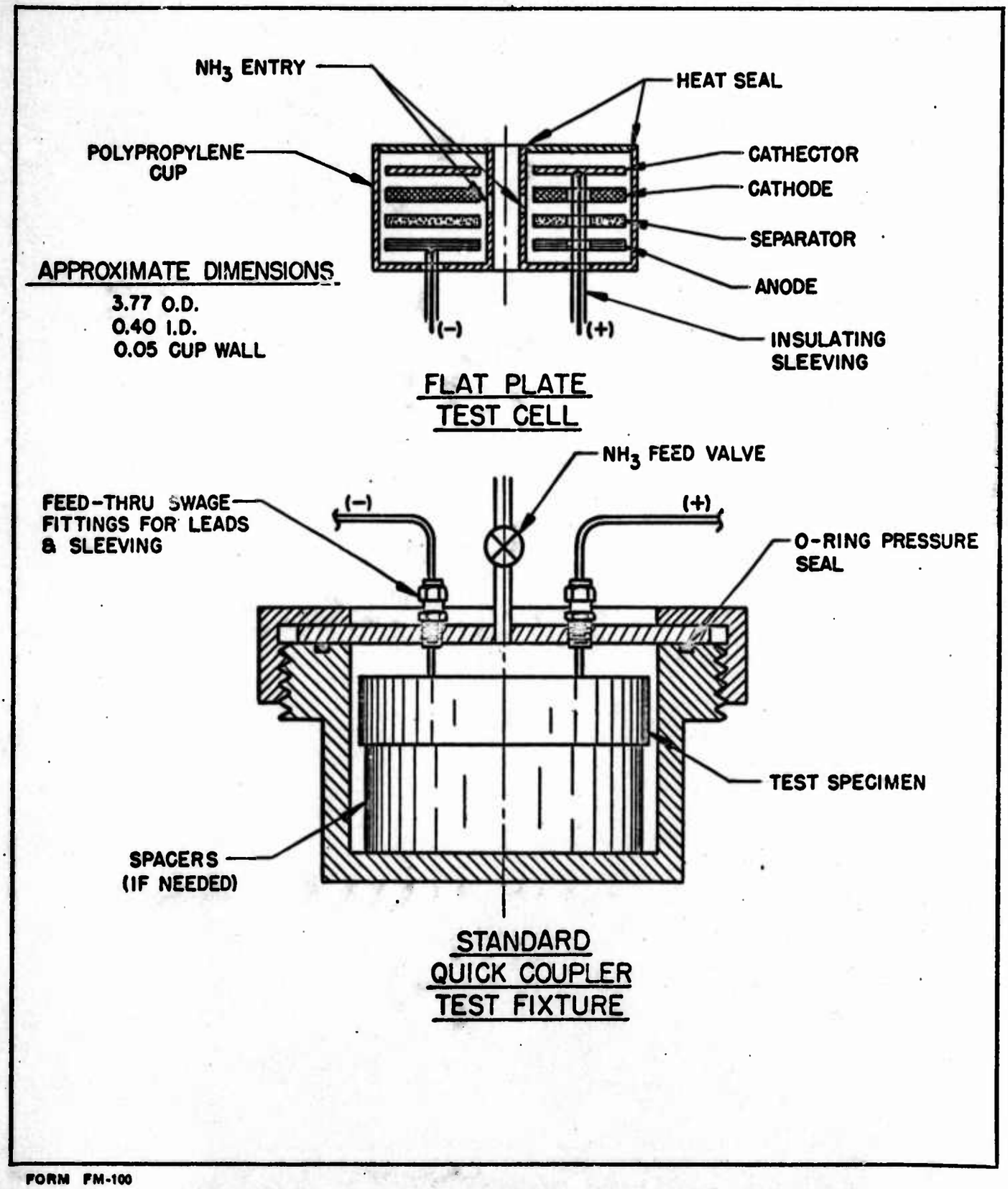

FORM FM-100

Figure C

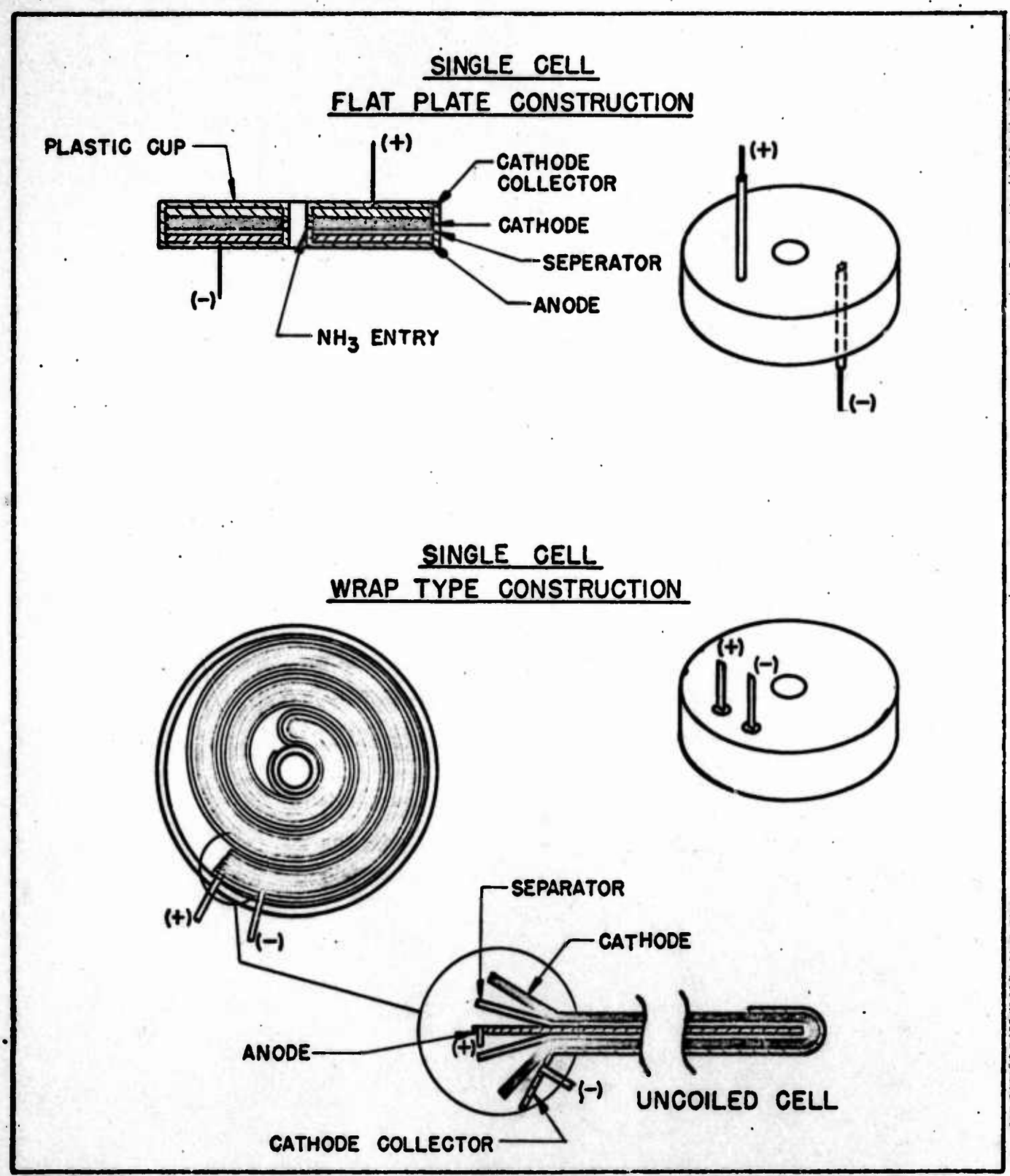

FORM FM-100

Figure D

Single Cell Construction

4.2.1 As the wrap-type cell was refined and tested in multicell stacks, it was found that a series of cells could be more easily assembled with alternate cells wrapped in reverse fashion as shown in Figure E. In this manner the wrap-type cells were stacked in series and bonded to the terminal plate as shown in Figure F.

(U) 4.3 Flat plate-type cells were judged on the basis of performance to be the better of the two configurations for this application. A parallel series arrangement, such as that shown in Figure G, was selected for use in multiple tests. This structure provides maximum cell working area within available space and offers relative construction simplicity.

4.3.1 Figure H, Engineering Drawing #72000541, shows an early design iteration of parallel cells in series, including tap connections. Series connections in this design were inside the cell stack. In the final design all connecting and tap leads are on the outside perimeter of the cell stack, except where they are welded to the cells, as shown in Figure I.

(U) 4.4 Testing in full stack (12 cells) subassembly format revealed problems in liquid distribution and thorough wetting of cell parts. This was largely due to the greater physical mass involved. In early designs and previous applications of the activation principles involved, a central liquid distribution manifold was employed. This did not prove to be satisfactory for the subject design.

4.4.1 Initial attempts to overcome distribution problems by means of increasing delivery pressures and velocities caused cell damage. Liquid ammonia entering the cell stack compartment built up excessive pressures in areas surrounding the input orifice.

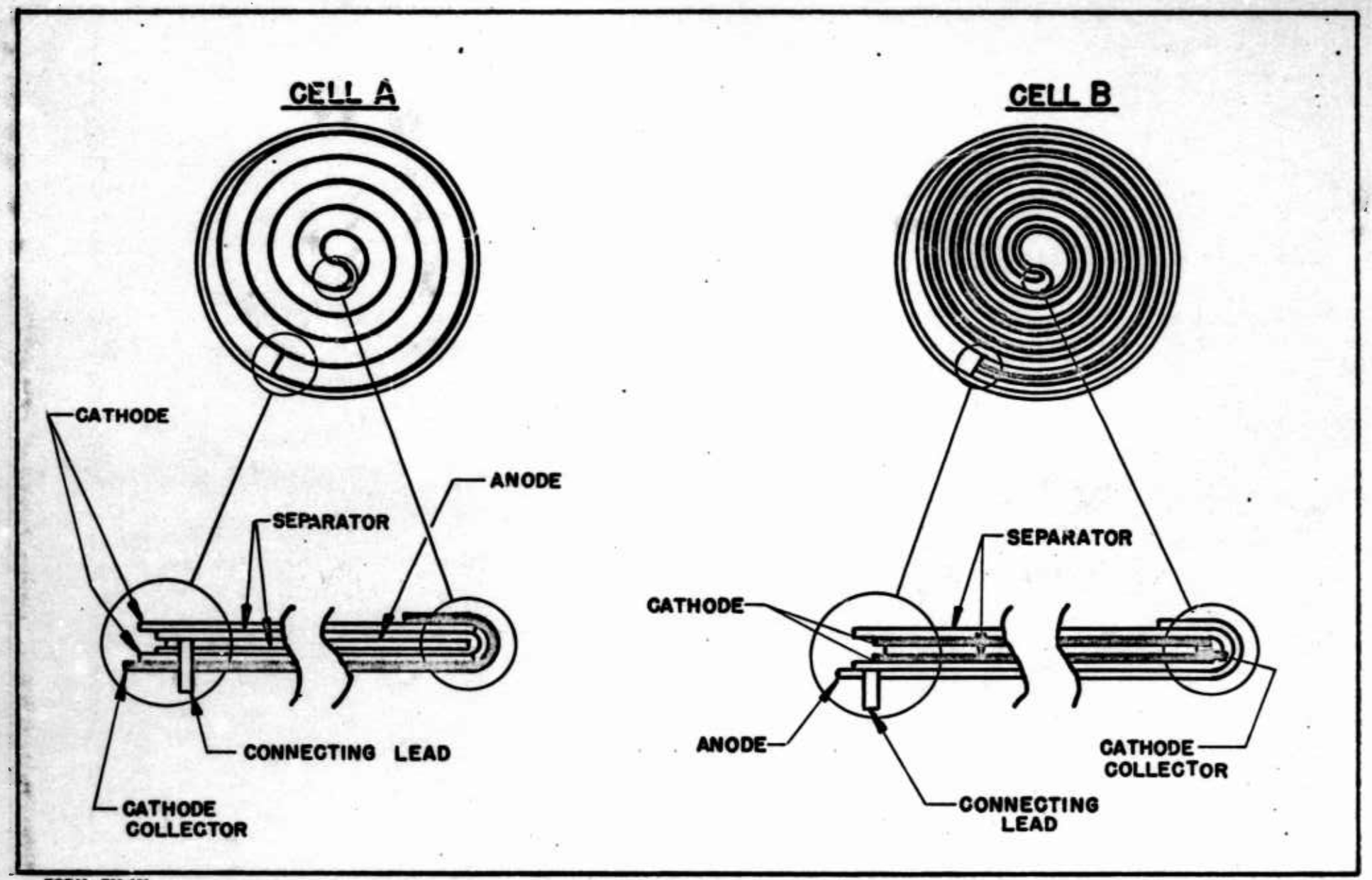

FORM FM-101

Figure E

Wrapped Cell Construction

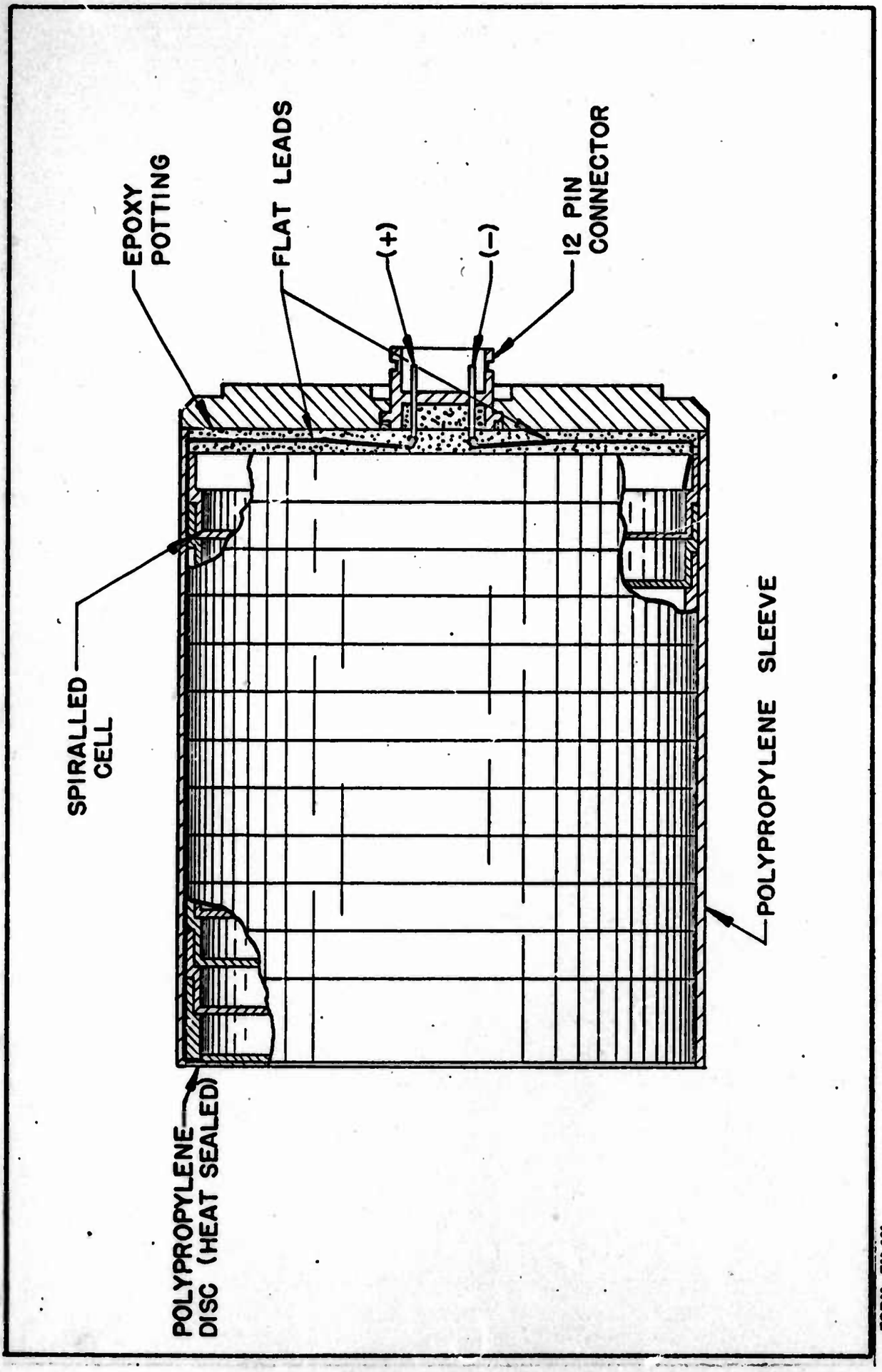

Figure F

Cell Stack

DRAWING NO. 7200038

BILL OF MATERIAL

ITEM	NAME	REQ.	PART NO.
1	CELL CUP	1	B-709
2	CATHODE	4	A-515
3	ANODE ASS'Y	1	A-536
4	COLLECTOR ASS'Y	1	A-534
5	SEPARATOR	4	A-522
6	INSULATION DISC	1	A-695

CONN
TAB,

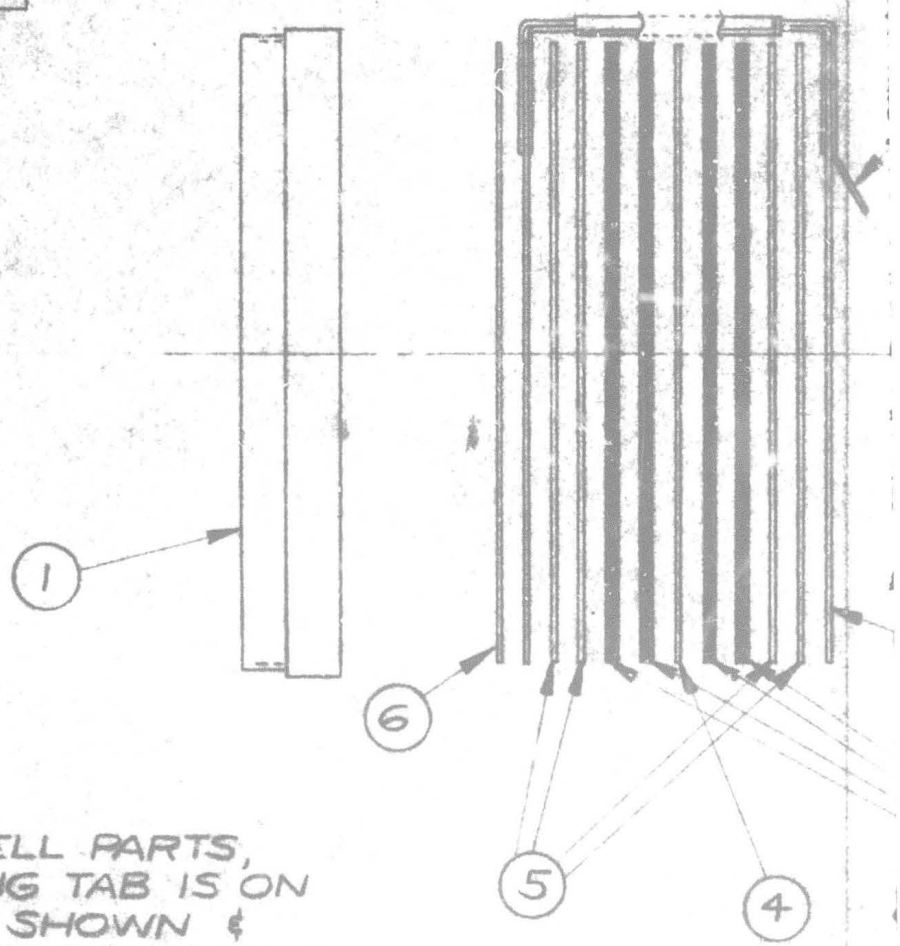

NOTES:

1-WHEN INSERTING CELL PARTS, BE SURE CONNECTING TAB IS ON ACCESSIBLE SIDE AS SHOWN & POSITIONED IN RELATION TO SLOT AS SHOWN.

2-INSERT COLLECTOR LEAD THRU SLOT AS SHOWN.

DO NOT SCALE DRAWING

ISSUE	REVISION
4	REDRAWN, REDES

FORM FM-109

A

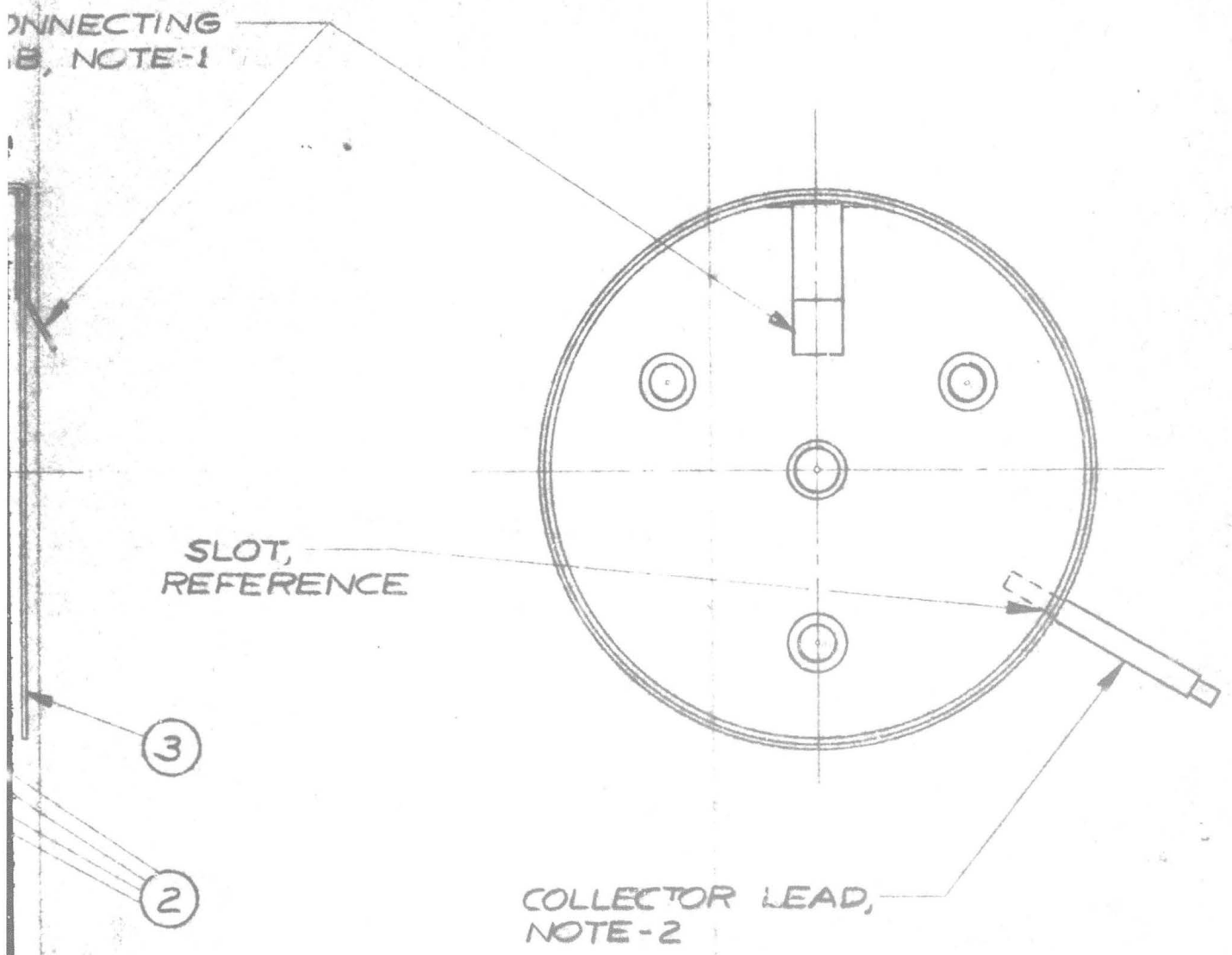

				TOLERANCES UNLESS OTHERWISE SPECIFIED:	LIVINGSTON ELECTRONIC CORP.						
				FRACTIONS ±	MONTGOMERYVILLE, PENNSYLVANIA						
				DECIMALS ±	DRAWN	DATE	CHECKED	DATE	APPROVED	DATE	
				ANGLES ±	AJG	7-26-67	JR	7-26-67			
					MATERIAL:				FINISH (WHERE NOT SPEC.)		
EDESIGNED	AJG	7-26-67		NEXT ASS'Y	SCALE	TITLE	CELL ASSEMBLY - INTERMEDIATE -		DRAWING NO.		
ON	BY	DATE	APPR		1/1				72000238		4

Figure G

B

[redacted]

BILL OF MATERIAL

ITEM	NAME	REQ.	PART NO.
1	CELL ASS'Y	1	B-537
2	CELL ASS'Y	4	B-538
3	CELL ASS'Y	3	B-538-1
4	CELL ASS'Y	3	B-538-2
5	INSULATION DISC	11	A-695
6	CELL CUP	1	B-708

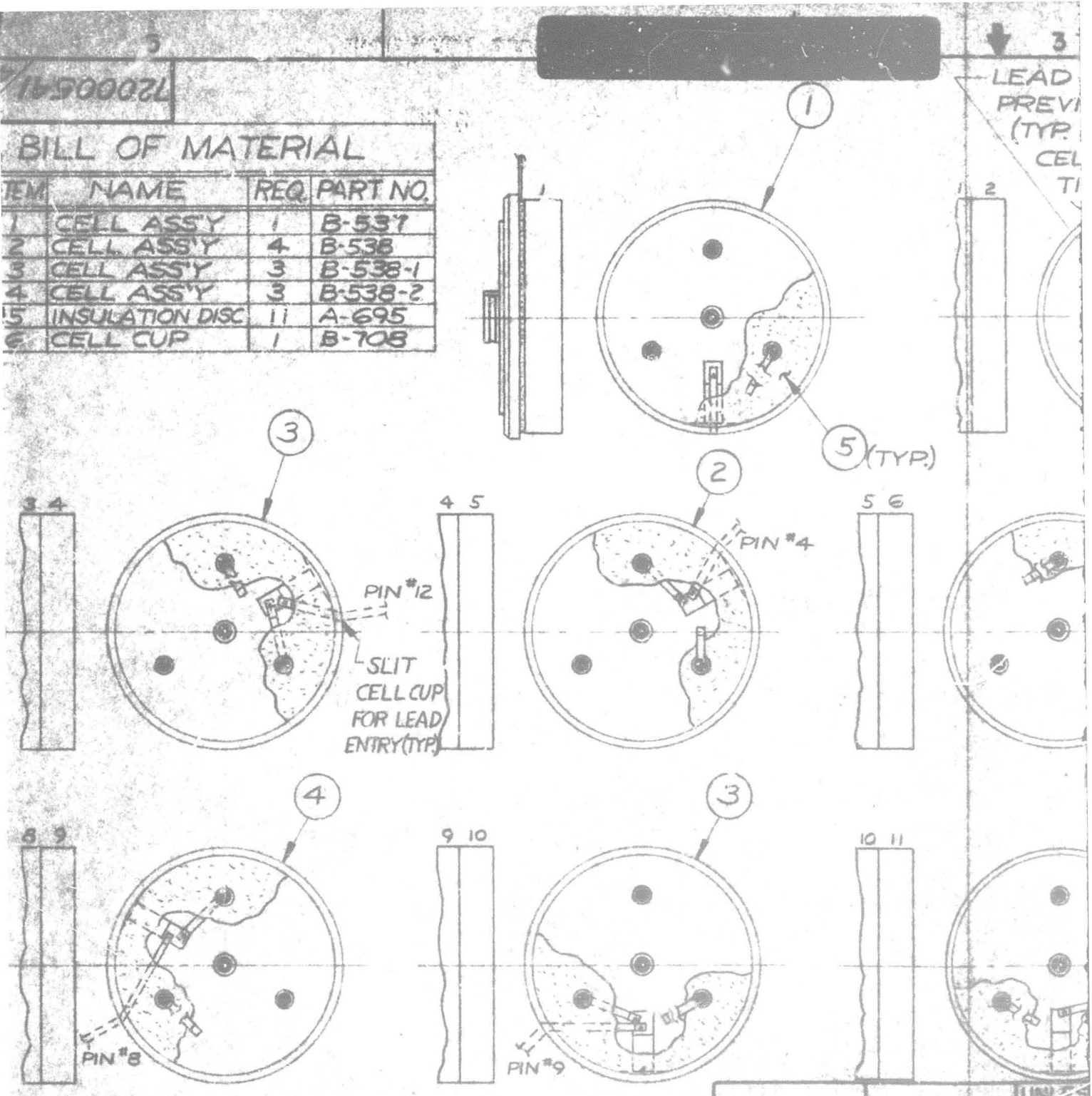

NOTES:
1- ALL LEAD CONNECTIONS SPOT-WELDED.
2- HEAT SEAL EACH CELL IN PLACE.
3- BE SURE THRU-HOLES ARE OPEN.
4- REFERENCE: SCHEMATIC A-544.

B-543	
NEXT ASS'Y	USE ON
APPLICATION	

UNLESS SPECIF
DEC
ANG
MATER

A

FORM FM-110

LEAD FROM PREVIOUS CELL (TYP ALL CELL TO CELL CONNECTIONS)

REVISION				
ZONE	NO.	DESCRIPTION	DATE	APPROVED
	3	REDRAWN & REVISED	9-23-65	
	4	B-708 WAS A-372	9-29-65	

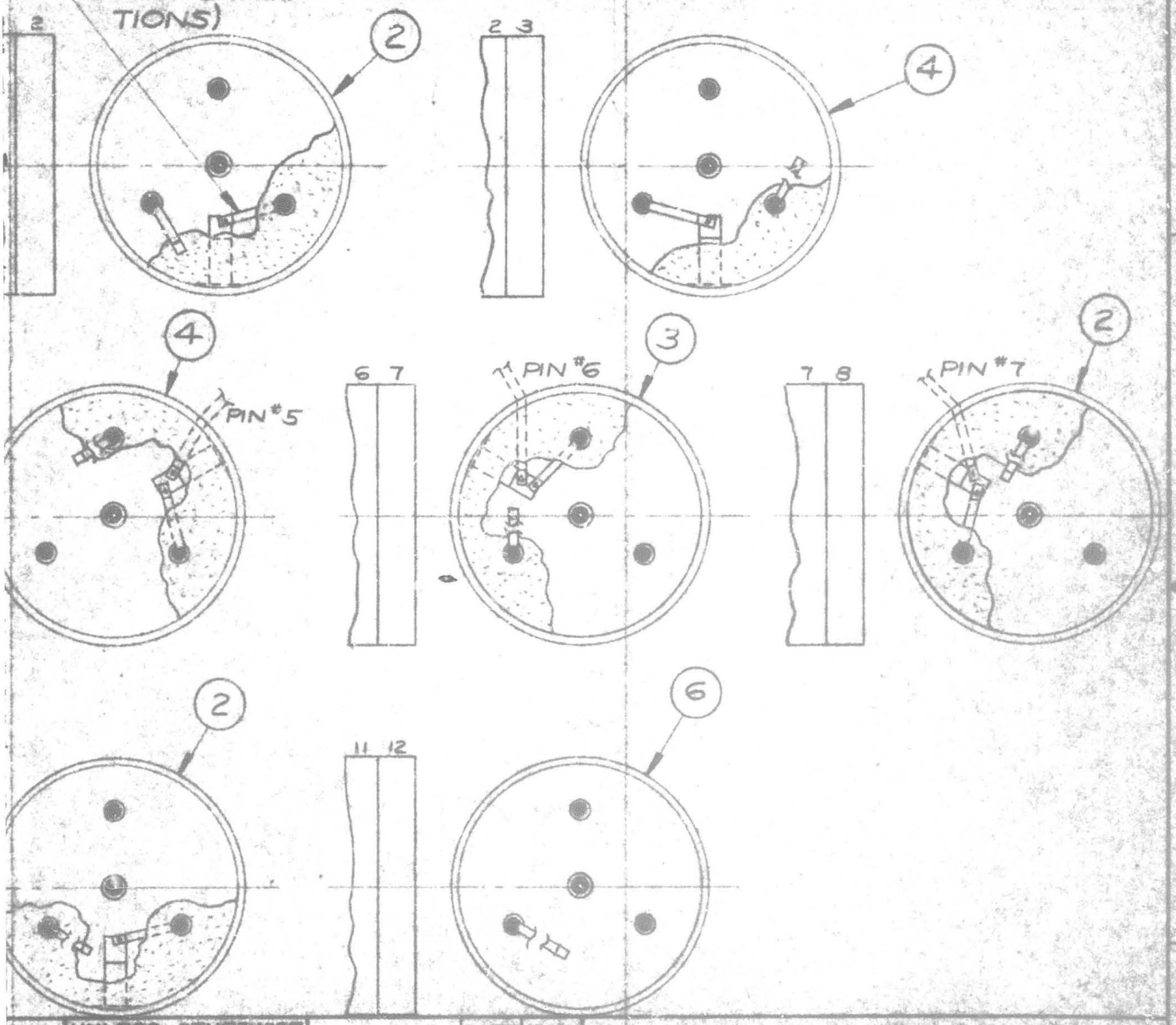

UNLESS OTHERWISE SPECIFIED: DECIMALS ± ANGLES ±		DATE	SIG.
MATERIAL	DRAWN	9-23-65	AJG
	CHECKED		
	APPROVED		

LIVINGSTON ELECTRONIC CORP.
MONTGOMERYVILLE, PENNA.

BATTERY BLOCK ASSEMBLY
— CELL STACK SEQUENCE —

SIZE B | CODE IDENT. 12 | 72000541

SCALE 1/1 | SHEET 1

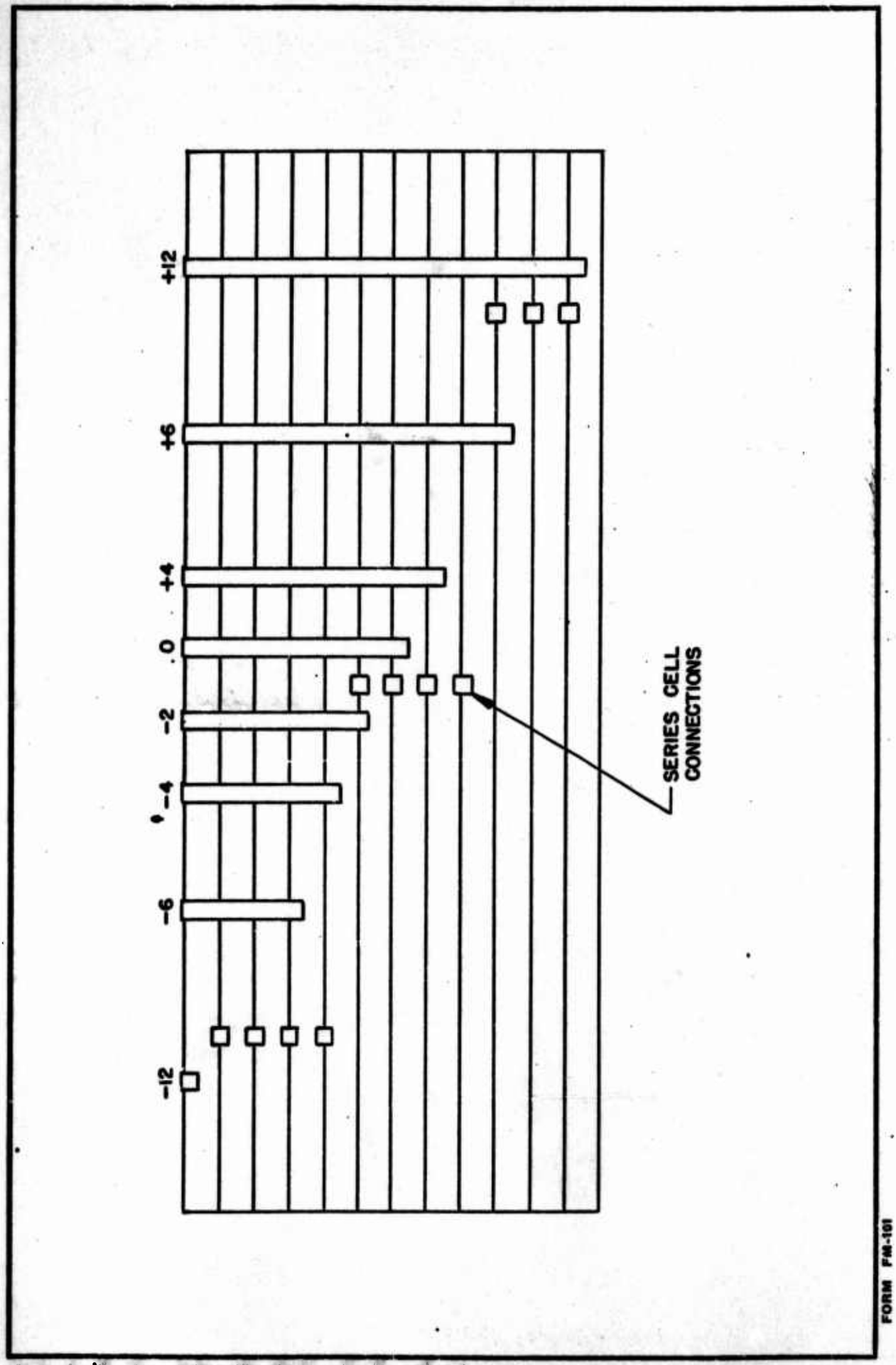

Figure I

Flat Tab Lead Arrangement

4.4.2 A means of minimizing damage caused by rapid liquid introduction was devised. A manifolding assembly consisting of three additional porting columns allows relatively fast equalization of pressure differentials, which develops when liquid is injected. An added advantage was observed in that the flow of liquid to cell area was found to be faster and more thorough.

4.4.3 One disadvantageous aspect to the approach was noted. This is the necessity of maintaining approximately four times as much void (nonenergy producing) volume within the cell stack. Standing columns of liquid allow more intimate points of potential internal electrical leakage. After considerable analysis, it was concluded that advantages of the approach outweighed the disadvantages and the metho was incorporated into the cell stack design.

(U) 4.5 In order to lend rigidity and strength to the cell stack, and in order to minimize free standing liquids in the manifold porting cavities, threaded nonconductive support rods were inserted for the full stack length in all four columns. This technique was found to greatly increase stack resistance to crushing, as well as offering the added advantage of a reduction in quantity of electrolyte required. Figure J illustrates this method.

4.5.1 At this time, connecting leads between individual cells were moved from inside the tubular distribution columns to a staggered arrangement externally located on the perimeter of the cell stack. (Reference Figure I, page #17)

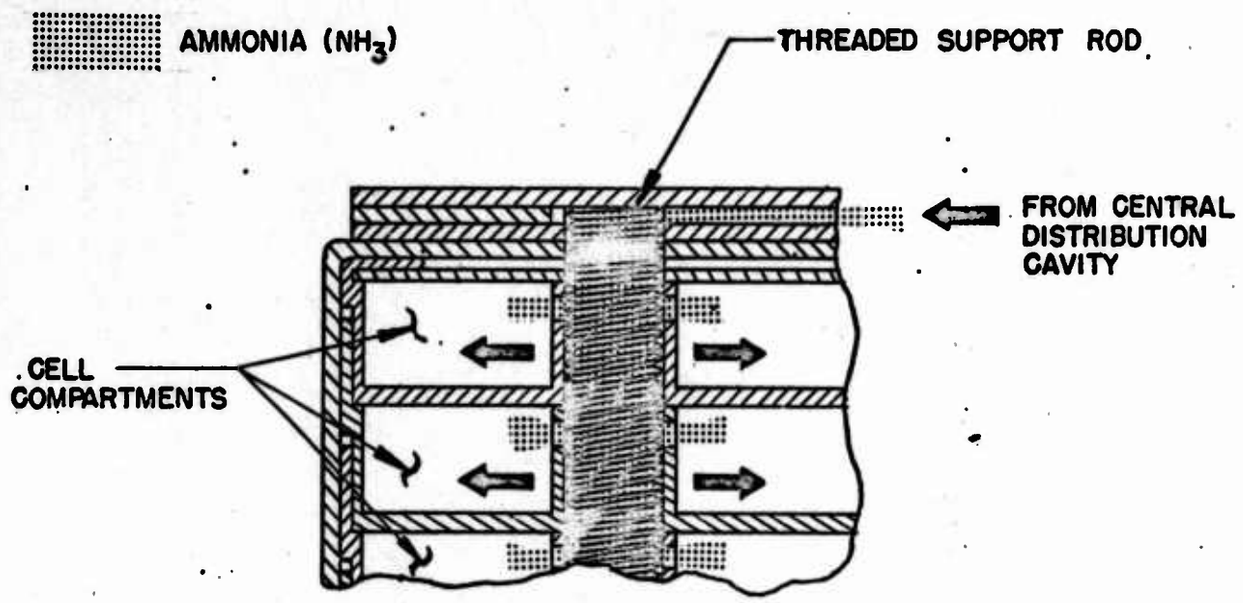

TYPICAL NH_3 ENTRY PATH

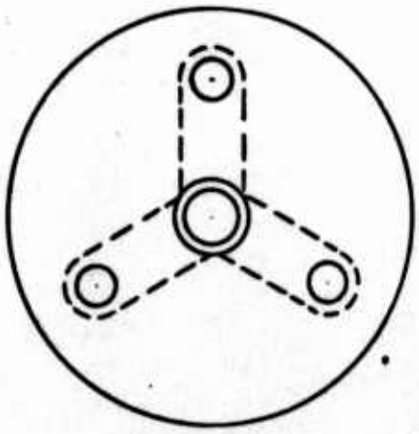

LOCATION OF SUPPORT RODS

FORM FM-100

Figure J

Activation Techniques

5.0 Activation Mechanism Design (U)

(U) 5.1 A major problem area undertaken throughout the program was the reliable transport of significantly larger quantities of electrolyte solvent than had ever been attempted before in reserve liquid ammonia batteries. The design of an activator cup which would perform such a function constituted a large portion of program efforts.

(U) 5.2 Operation of the activation mechanism is dependent upon several basic principles.

5.2.1 In the reserve state the unit must be capable of withstanding the vapor pressure of liquid anhydrous ammonia across the entire storage temperature range. Because vapor pressures at positive temperatures in this range require substantial structures for containment, a folding cup or bellows requires external mechanical containment in the form of the outer battery case.

5.2.2 The liquid reservoir (bellows or inner cup) must allow sufficient internal volume to permit volumetric expansion of liquid ammonia with respect to temperature. An appropriate volume of liquid to completely fill the void space in the cell stack at the most dense condition must also be included. Liquid ammonia expands volumetrically approximately 35% in the specified temperature range.

5.2.2.1 A safety factor of 10% minimum has been allowed to avoid the potential hazard of bursting the reservoir cup hydrostatically in the event of an unintentional exposure to temperatures beyond storage specification.

5.2.3 When gas pressure is generated within the space between the reservoir cup and the outer case walls, the cup tends to collapse against the gas pressure within until a hydrostatic condition prevails. At that point a

burst diaphragm in the bulkhead is scheduled to release liquid out of the reservoir. Cup deformation must therefore be of such a nature as to accommodate the physical properties and principles described. Improper deformation causes poor battery performance by virtue of incomplete activation of cells.

(U) 5.3 Six complete design iterations were undergone. This involved the total evolution of each successive iteration all the way to test and evaluation in prototype batteries. Although means were investigated which might allow a preliminary qualification for this vital aspect of the battery package, no satisfactory qualifying criteria could be established short of complete battery testing.

5.3.1 Design #1 as shown in Figure K used a straight side wall. Although this principle has been successfully used in smaller battery units, the deformation proved very irregular resulting in cracks and tears.

5.3.2 Design #2 employed a sliding guide ring, also used in previous work. Although a definite improvement was evident, insufficient delivery travel was achieved resulting in low quantity delivery. Increased pressures were rejected as being in excess of outer case safety limits.

5.3.3 Design #3 using a conventional bellows arrangement functioned satisfactorily only when pressure was applied in a steady increasing fashion. As the gas generator force is not applied in this fashion, but is produced nonlinearly with time, this approach was rejected upon continuous occurrence of leakage.

5.3.4 Design #4 inverted the principles involved in previous work, making the gas pressure expand the bellows rather than compress it. Here again the nonuniform pressure rise caused leaks in sections of the cup hardened by expansion movement.

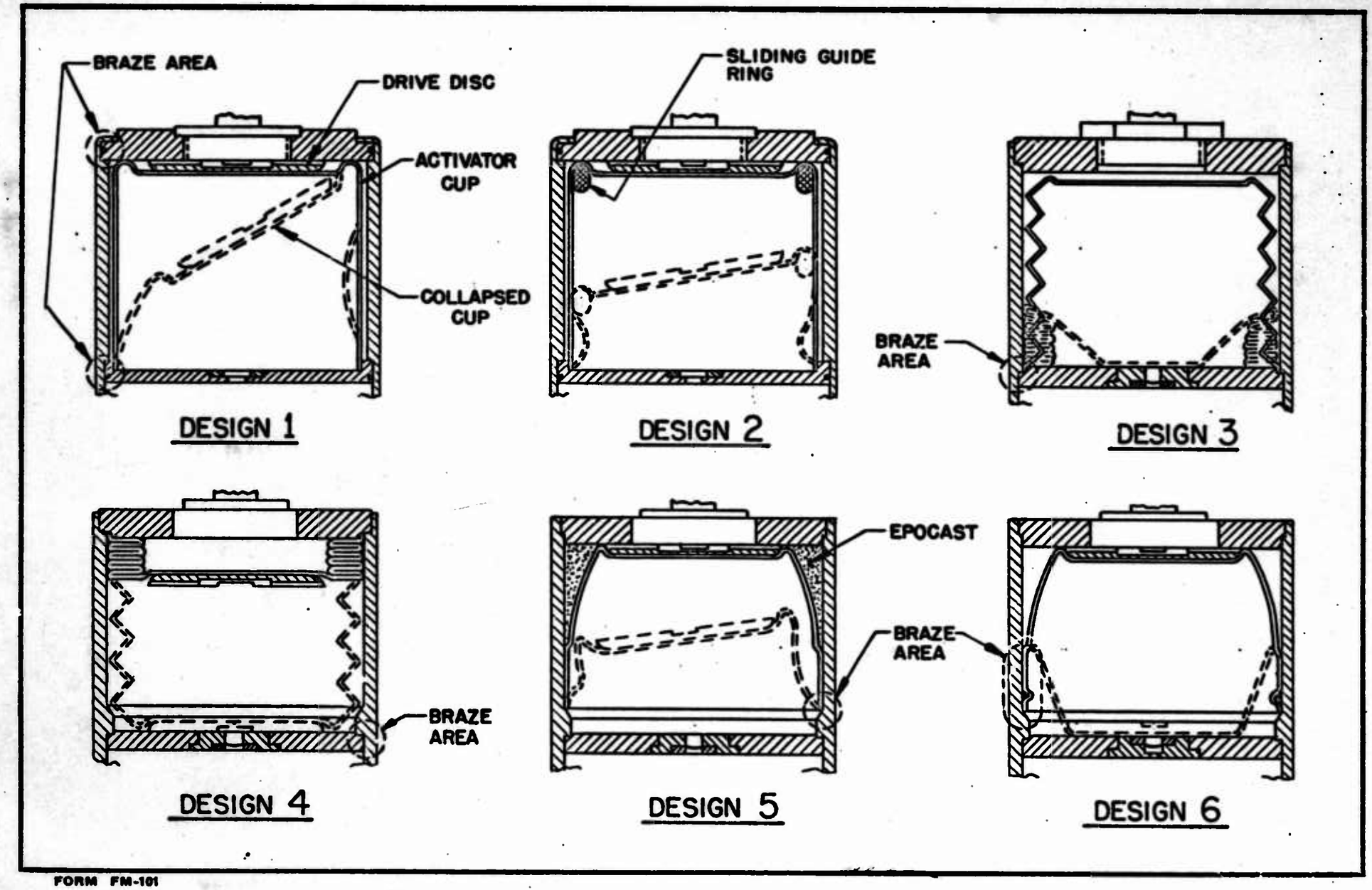

FORM FM-101

Figure K

Activator Cup Design Iterations

5.3.5 Design #5 made use of a domed cup supported in a rest position by a potting material. A high braze area as illustrated in Figure K had the effect of strengthening side walls. This approach was found to function satisfactorily but not efficiently in terms of delivery. Liquid content had to be increased at cold temperatures, which resulted in insufficient expansion factors at high temperatures. Experimentation with this design did, however, lead to the final and most satisfactory design.

5.3.6 Design #6 has been successfully employed on final prototypes. A higher anchor position and a carefully controlled braze level allow an efficient cup.

5.3.6.1 The use of potting compound was discontinued when test results indicated little or no functional purpose was being served.

(U) 5.4 To determine proper cup wall thickness in relation to deformation pressures involved, a series of quantitative determinations was made by hydraulic pressure tests. Since gas generator pressures behind the ammonia cup during the activation sequence must exert sufficient force to deform the reservoir cup itself as well as delivery of contents, it follows that design pressures should be the minimum necessary to obtain proper deformation. Table 1 shows results of such testing.

TABLE 1

Ammonia Cup Deformation

Wall Thickness	Pounds/Force								
	50-100	100-150	150-200	200-250	250-300	300-350	350-400	400-450	Above 450
0.033"								1	5
0.032"							2	3	1
0.030"						2	4		
0.028"						5	1		
0.024"				5	1				
0.021"			3	3					
0.019"		6							

6.0 Gas Generator Design (U)

(U) 6.1 The gas generator, as employed in the battery activator, serves a dual function. The activator cup (bellows) must be depressed by pyrotechnic gas products of sufficiently high pressure to deform the cup, and the gaseous products must be sufficiently persistent to keep the cup collapsed against variable ammonia back-pressure, which relates to environmental temperature.

(U) 6.2 A three-stage pyrotechnic chain has been used, consisting of a percussion primer of the M5 variety, a fast burning igniter material, and a relatively fast burning propellant material.

6.2.1 Early designs were set up using a double-base propellant material. During the course of the program a materials selection shift to slower burning, more stable gas generating propellant proved to reduce initial peak pressures developed.

(U) 6.3 Components of the gas generator assembly are illustrated in Figure L, showing two design iterations. In order to reduce gas pressure peaks, reductions in burning rate were effected by reducing the surface ignition area. Triangular shaped center holes were rounded, and igniter quantity was reduced. A more restrictive baffle was introduced as a means of limiting the delivery rate of gas produced.

6.3.1 Gas generator units were initially proven in test bomb fixtures with void space equivalent to a collapsed activation cup. Once basic parametrics were established, however, it became necessary to test gas generators in pieces of activator hardware loaded with liquid in order to obtain proper simulation of actual operating conditions.

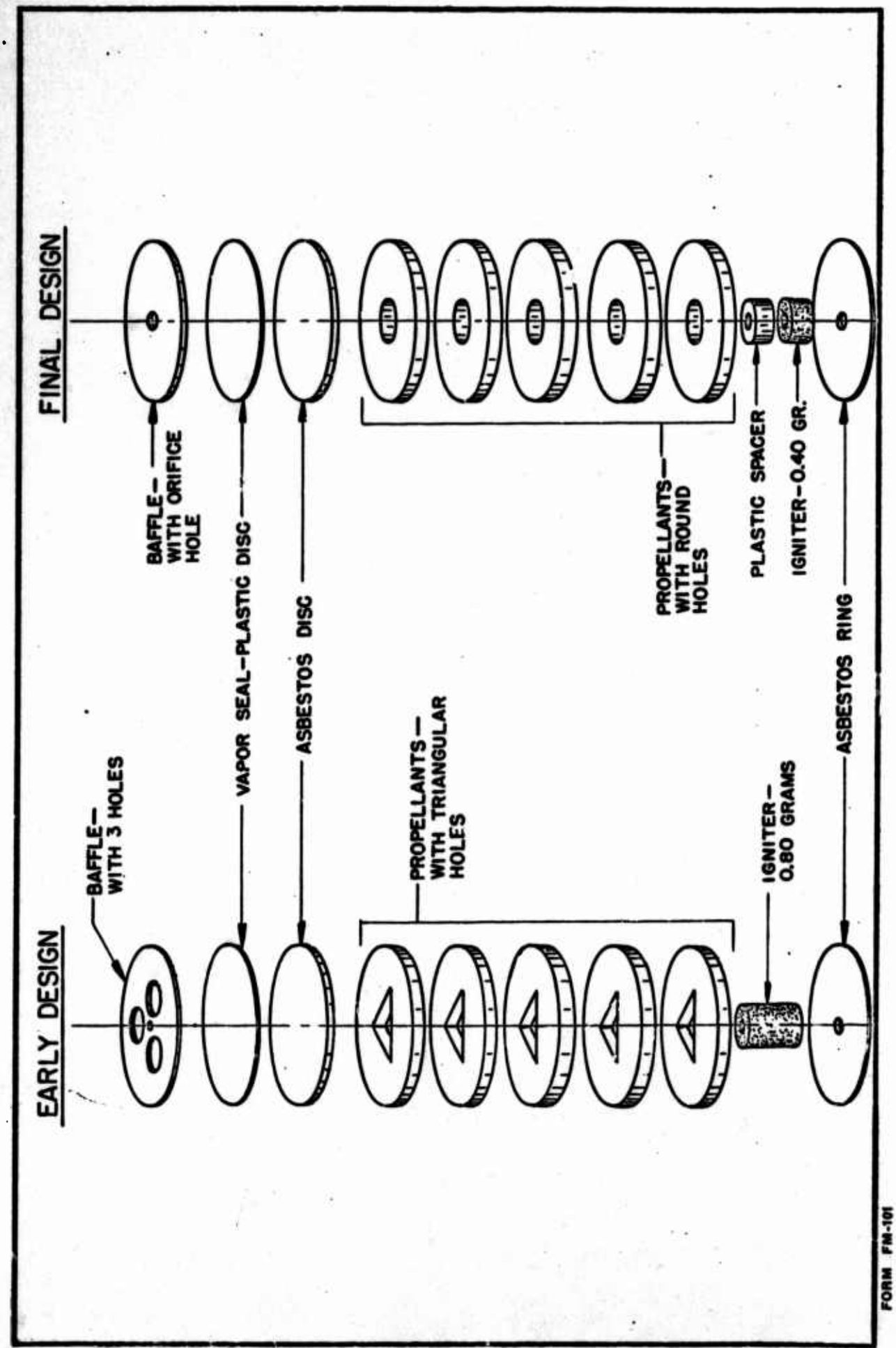

Figure L

Gas Generator Components

(U) 6.4 Early test results showed an initial high peak of pressure in the order of milliseconds after ignition reaching peaks of 1800 psi. A very rapid decline then took place, leaving a residual pressure in the range of 600 psi. A burning rate adjustment having been made, the same minimum necessary quantity of propellant material was observed to present a lower peak pressure in the order of one second after activation in a less abrupt fashion.

6.4.1 Tests were conducted using transducers ported in such a fashion that pressure readings were being recorded behind the collapsible activator reservoir cup or bellows. Such testing and adjustment was done for each cup configuration previously mentioned (paragraph 5.3 this report). Figure M shows a typical test and result profile for one of the cup design studies.

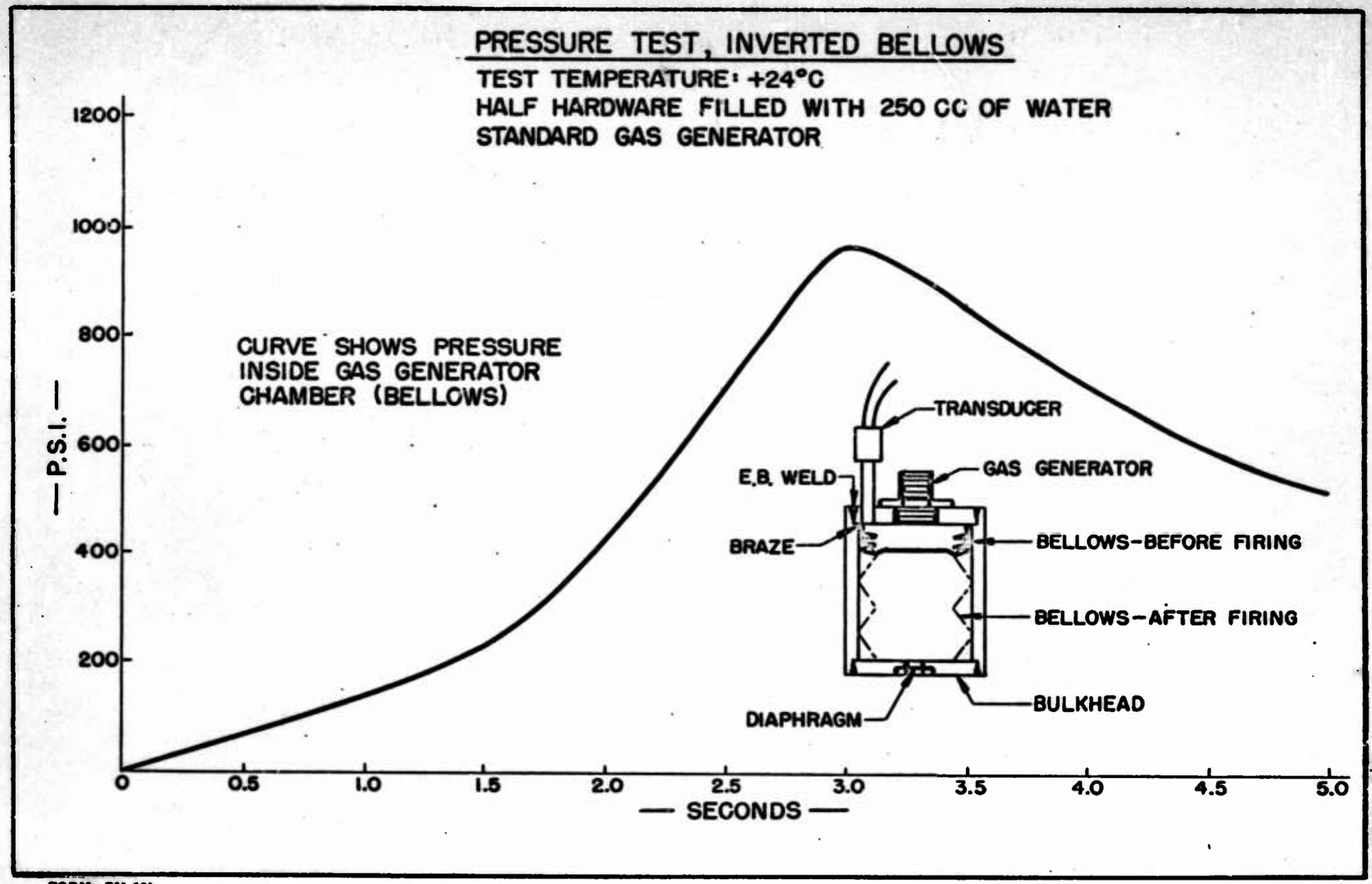

FORM FM-101

Figure M

Pressure Data

7.0 Ammonia Delivery Controls (U)

(U) 7.1 The pressure at which ammonia is delivered through the bulkhead orifice is controlled by the following factors: the burning rate and gas pressure buildup in the gas generator chamber, the pressure at which the bulkhead diaphragm will rupture, size of the bulkhead orifice, and the size and number of ammonia feed columns and ports in the cell stack.

(U) 7.2 Stages in the development of the bulkhead diaphragm assembly are illustrated in Figure N.

7.2.1 In Design "A," the diaphragm was a punched steel disc held in the bulkhead assembly by a retaining ring. With this approach it was not possible to subject sample diaphragm assemblies to advance pressure tests. This was because of the fact the retaining ring was secured in the bulkhead assembly by brazing in the same operation that the bulkhead assembly itself was brazed into the battery tube. As a result some of the bulkhead diaphragms ruptured prematurely under the ammonia vapor pressures generated at the high temperature limit. Lack of reliability mandated further design consideration.

7.2.2 Advance pressure testing was made possible with adoption of Design "B" (Figure N), in which a punched stainless steel diaphragm disc was electron beam welded to the diaphragm holder. With this approach, individual lots of diaphragm assemblies were pressure tested in advance, and specified numbers of sample diaphragm assemblies were ruptured to establish reliability data. It was experimentally determined that higher rupture pressures could be achieved, without increased thickness, by annealing and Teflon coating the stainless steel parts. As a means of avoiding attrition from stresses set up in the punching operation, Design "B" diaphragms were punched oversize and then machined to the proper diameter.

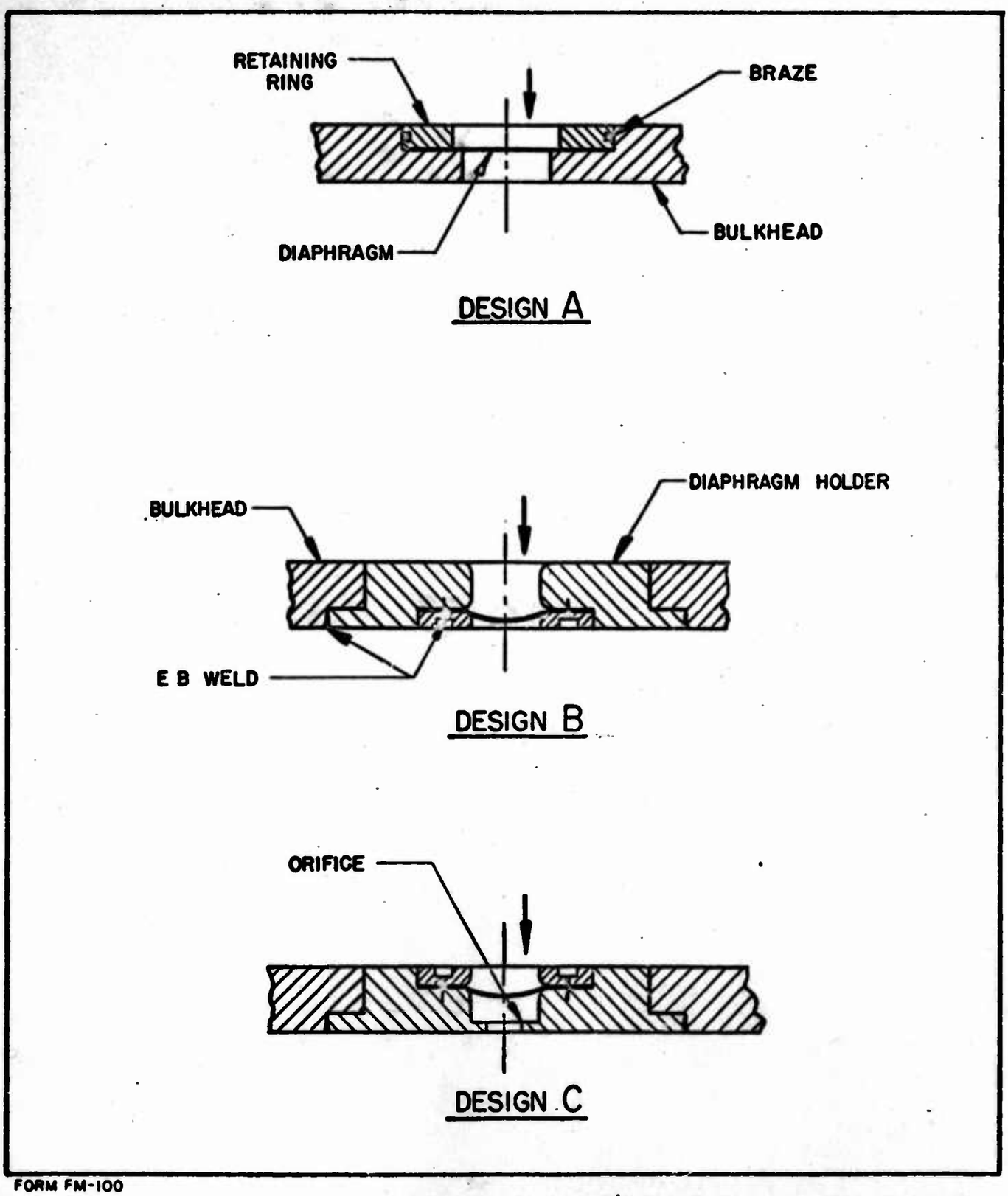

FORM FM-100

Figure N

Bulkhead Diaphragm Iterations

7.2.3 Stresses that might be set up by the punching and machining operations were eliminated with the change over to Design "C" (Figure N), the current design. In this case the diaphragm is formed by a photographic etching process.

7.2.4 Additional modifications were introduced into Design "C." The bulkhead orifice diameter was decreased, while the rupture pressure characteristics were held between 680 and 720 psi. This has had the effect of softening the flow of liquid, although velocity is increased.

(U) 7.3 Pressure relationship studies were conducted in order to optimize activation and operating pressures. Figure O shows final design characteristics with diaphragm burst at approximately 640 psi and retention pressures somewhat less than 400 psi. Battery compartment (cell) operating pressures, as well as activation pressures, were measured with transducer monitoring devices located in various positions on operational battery models.

7.3.1 Tests made using water, as well as ammonia, as a transport medium were used to ascertain pressure characteristics. Table 2 shows results obtained with such tests.

TABLE 2

Trial	Medium *	Diaphragm	Diameter Breakthrough	Break Pressure	Retention Pressure
1	H_2O	0.0015"	0.238"	605	300
2	H_2O	0.0015"	0.238"	614	310
3	H_2O	0.0015"	0.238"	613	328
4	NH_3	0.0015"	0.238"	633	330
5	NH_3	0.0015"	0.238"	641	351

* Units containing H_2O were further pressurized to a 125 vapor pressure in order to compare with the NH_3 conditions.

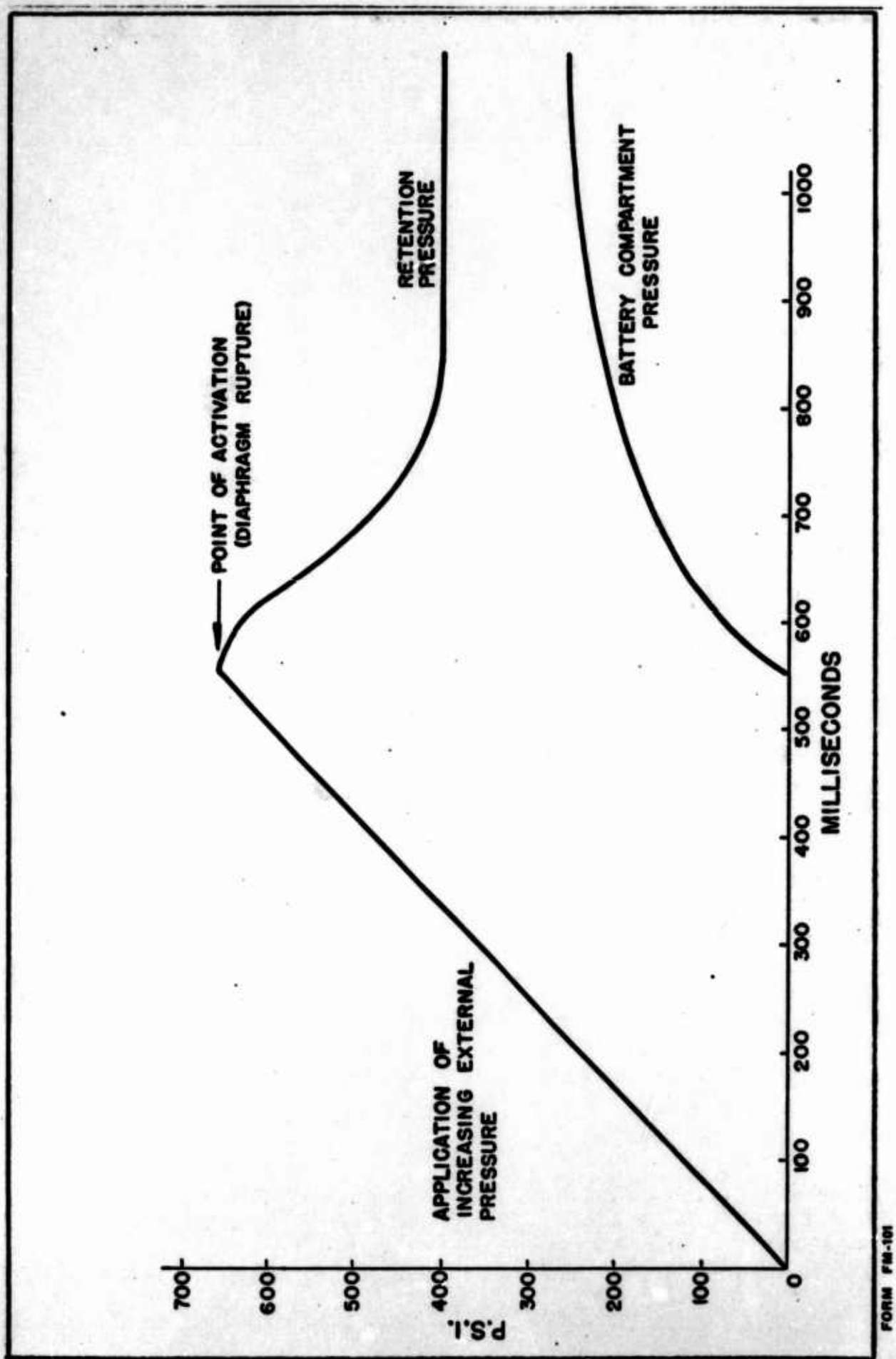

Figure O

Pressure Characteristics

8.0 Insulating Leads and Terminal Pins (U)

(U) 8.1 A major subject area of technical difficulty persisting throughout much of the program involved finding satisfactory methods by which the numerous electrical leads could be isolated from one another. Because output taps are required to present different cell voltages, each lead wire and terminal pin must be isolated electrically from one another as well as isolated from the common conductive electrolyte.

(U) 8.2 For volumetric efficiency, flat tab lead wires are used between individual cells (reference Figure I) as well as from cells and groups of cells to output terminal pins. Difficulty was encountered in attempts to insulate the flat wires because of the corrosive effect of the electrolyte solutions, which allowed intermittent internal shorting between cells.

8.2.1 Teflon and glass coating materials proved effective for shorter intervals than the required discharge period. A double layer of Teflon wrapped in an overlay fashion has, however, added sufficient isolation to lead wires to give the necessary protection.

(U) 8.3 A similar, but separate problem, which appears to have been satisfactorily resolved, involved effective isolation of the terminal pins within the battery. In this regard, the original specifications had called for the terminal plug or header to be placed in the center of the terminal plate. With such an arrangement, satisfactory isolation of the leads from the terminal plate was accomplished by wrapping the radially spaced leads with Teflon tape and then potting them in silicone rubber and epoxy.

8.3.1 A subsequent modification called for the terminal plug or header to be offset to the side, and not centered in the terminal plate. When this change was effected, it was found that potting in epoxy did not effectively isolate them

throughout battery life. New potting materials and techniques were examined, and a strict fabrication process was devised which gave satisfactory results.

8.3.2 With introduction of latter methods and materials it was also reasoned that less shorting would be likely to occur if the electrical potential could be kept to a minimum between terminal pins in close proximity to one another. In Figure P a new arrangement of tap leads is shown, together with the former arrangement, in which tap leads with highest electrical potential were located in closer proximity to one another.

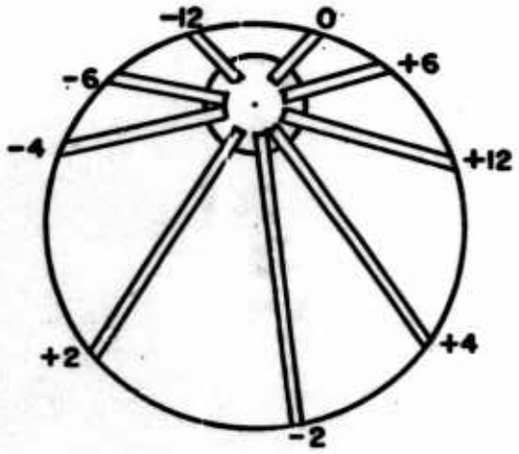

FORMER

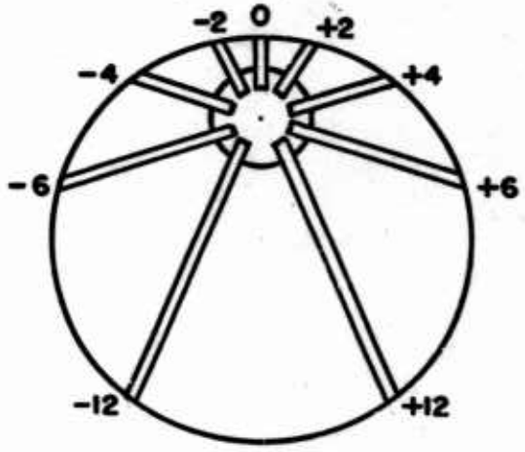

LATTER

FORM FM-101

Figure P

Terminal Plate Lead Arrangement

9.0 Safety Diaphragm (U)

(U) 9.1 Internal short circuits within the battery have been observed to develop from relatively obscure and minute breakdown of insulation surfaces. This has been observed to frequently affect only one cell, and in so doing does not detract significantly from the total energy capacity of the total battery.

(U) 9.2 When small internal short circuits, more appropriately defined as intercell leakage, become sufficiently gross to expend battery energy as heat, a potentially hazardous condition could prevail. Heat, if sufficiently high, has a regenerative effect, in that further breakdown from heating causes more shorting which causes more heat. In such a fashion it is possible that a battery suffering severe internal damage could build up sufficient pressure to rupture the sealed case.

9.2.1 In several prototype battery tests such a situation did occur, causing some damage to environmental equipment. The rupture event is a pressure venting circumstance, not an explosion in the pyrotechnic sense. Even so the possibility of such an event was judged not to be acceptable.

(U) 9.3 For purposes of pressure relief, should an unexpected condition create an overpressure within the sealed battery, a safety diaphragm was included in the terminal plate. This subassembly, preset to rupture at 1500 psi, was designed to relieve overpressure at a moderately slow rate. Because case structure and seals were designed and tested to approximately 12,000 psi, a safety factor of significant magnitude was provided against a catastrophic-type battery failure.

9.3.1 Table 3 represents typical test data from which safety vent design was derived.

TABLE 3

Safety Vent Investigation

Test Date	Material	Thickness	Diameter	Hardness	Teflon Coated	Rupture Pressure
2/19/67	SS	.001"	.200"	Annealed	Yes	975 psi
2/19/67	SS	.001"	.200"	"	Yes	975 psi
2/19/67	SS	.001"	.200"	"	Yes	950 psi
2/19/67	SS	.001"	.200"	"	Yes	1000 psi
2/19/67	SS	.001"	.220"	"	Yes	1050 psi
2/19/67	SS	.001"	.220"	"	Yes	950 psi
2/19/67	SS	.003"	.240"	"	Yes	2300 psi
2/24/67	SS	.002"	.200"	"	Yes	3000 psi *
2/24/67	SS	.002"	.200"	"	Yes	3000 psi *
2/24/67	SS	.002"	.200"	"	Yes	3000 psi *
2/24/67	SS	.002"	.220"	"	Yes	3000 psi *
2/24/67	SS	.002"	.220"	"	Yes	3000 psi *
2/24/67	SS	.002"	.220"	"	Yes	3000 psi *
2/24/67	SS	.002"	.240"	"	Yes	2700 psi
2/24/67	SS	.002"	.240"	"	Yes	2775 psi
2/24/67	SS	.002"	.240"	"	Yes	-
2/24/67	SS	.002"	.260"	"	Yes	2300 psi
2/24/67	SS	.002"	.260"	"	Yes	2350 psi
2/24/67	SS	.002"	.260"	"	Yes	2300 psi
2/24/67	SS	.002"	.310"	"	Yes	1700 psi
2/24/67	SS	.002"	.310"	"	Yes	1675 psi
3/03/67	SS	.0015"	.200"	50% Work Hard.	Yes	2650 psi
3/03/67	SS	.0015"	.200"	"	Yes	2775 psi
3/03/67	SS	.0015"	.200"	"	Yes	2900 psi
3/03/67	SS	.0015"	.220"	"	Yes	2300 psi
3/03/67	SS	.0015"	.220"	"	Yes	2500 psi
3/03/67	SS	.0015"	.220"	"	Yes	2500 psi
3/03/67	SS	.0015"	.240"	"	Yes	1900 psi
3/03/67	SS	.0015"	.240"	"	Yes	1850 psi
3/03/67	SS	.0015"	.240"	"	Yes	1825 psi
3/03/67	SS	.0015"	.260"	"	Yes	1800 psi
3/03/67	SS	.0015"	.260"	"	Yes	1700 psi
3/03/67	SS	.0015"	.260"	"	Yes	1750 psi

not rupture.

10.0 Final Seal Techniques (U)

(U) 10.1 Figure Q illustrates the three different methods used successively to effect the seals of the top cap and terminal plate to the tube. The Design "C" techniques represent final design.

(U) 10.2 Design "A" was first employed on early test hardware. The mechanical closure was in this case a rolled metal lip, while the seal was provided by a braze ring on the top cap and an epoxy seal on the final or terminal plate end. Insufficient structural strength was provided.

(U) 10.3 Design "B" employed heliarc welding beads along seal perimeters on both ends of the battery. Although structurally this method was satisfactory, the high heat imparted by heliarc welding caused battery components to be damaged within the unit.

(U) 10.4 Design "C," using a press fit assembly which is joined by all around electron beam weld beads, was found to be satisfactory.

10.4.1 Some difficulty was experienced in obtaining access to electron beam equipment of sufficient size, power, and precision to handle the battery case, which is relatively large for this particular type of weld. These welding difficulties and the associated very high service costs eventually resulted in the purchase and modification of electron beam welding equipment as Honeywell-owned capital items.

(U) 10.5 Originally, the gas generator assembly was threaded into the top cap and epoxy sealed. This method eventually was eliminated in favor of a press fit with the parts electron beam welded.

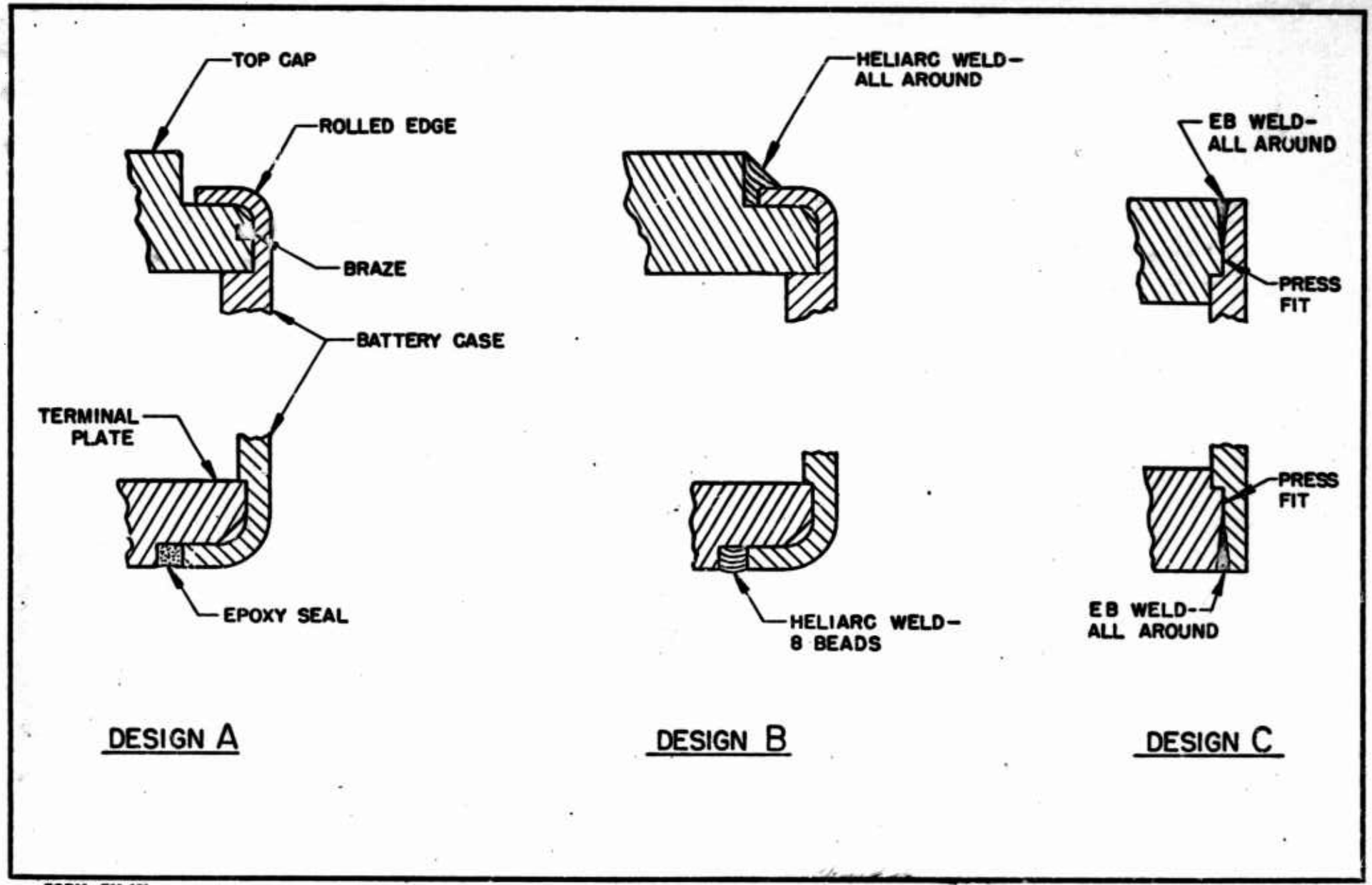

Figure Q

Sealing Iterations

11.0 Performance Summary (U)

(U) 11.1 Batteries have been tested for various experimental evaluations either in a full hardware state or in a subassembly cell stack mode. The latter test circumstance has been referenced as "half hardware," indicating that the integral activating mechanism was not fired (the battery being activated from an external source).

(U) 11.2 In the course of evaluation of packaging methods, test results have frequently shown partial operation of batteries. Although a full stack consists of 24 volts (12 cells), loading is applied across individual cells reading from a 0-volt center tap to +12, +6, +4, +2 volts. Likewise, -12, -6, -4, and -2-volt taps are monitored. When mechanical packaging difficulties occur in a given portion of a cell stack, the effect is such that the 24-volt potential reflects changes not always associated with individual tapped sections. An example is shown in Figure R, where the test specimen showed satisfactory performance on just half the voltage taps being monitored. Subsequent analysis showed a packaging deficiency in one cell only.

(U) 11.3 Operational requirements have been met at all temperatures with respect to discharge life. Voltage levels, however, drop below required minimums during the superimposed pulse loading (operate load) at the end of discharge life. Table 4 summarizes typical performance at different temperature levels.

TABLE 4

Unit No.	Test Temp.	Peak Voltage	Hours to 21.6 v	Operating Load Pulse Hours	Volts	Hours	Volts
13G	-65°F	28.1	59.0	-	-	48	23.8
10G	+72°F	28.2	136.0	24	19.3	48	18.7
F21	+125°F	28.9	109.5	24	19.5	50	18.1
11G	+160°F	28.2	19.0 *	24	17.0	48	18.2

* When operating load applied at 24 hours voltage recovered to above 21.6 and ran out to 130 hours.

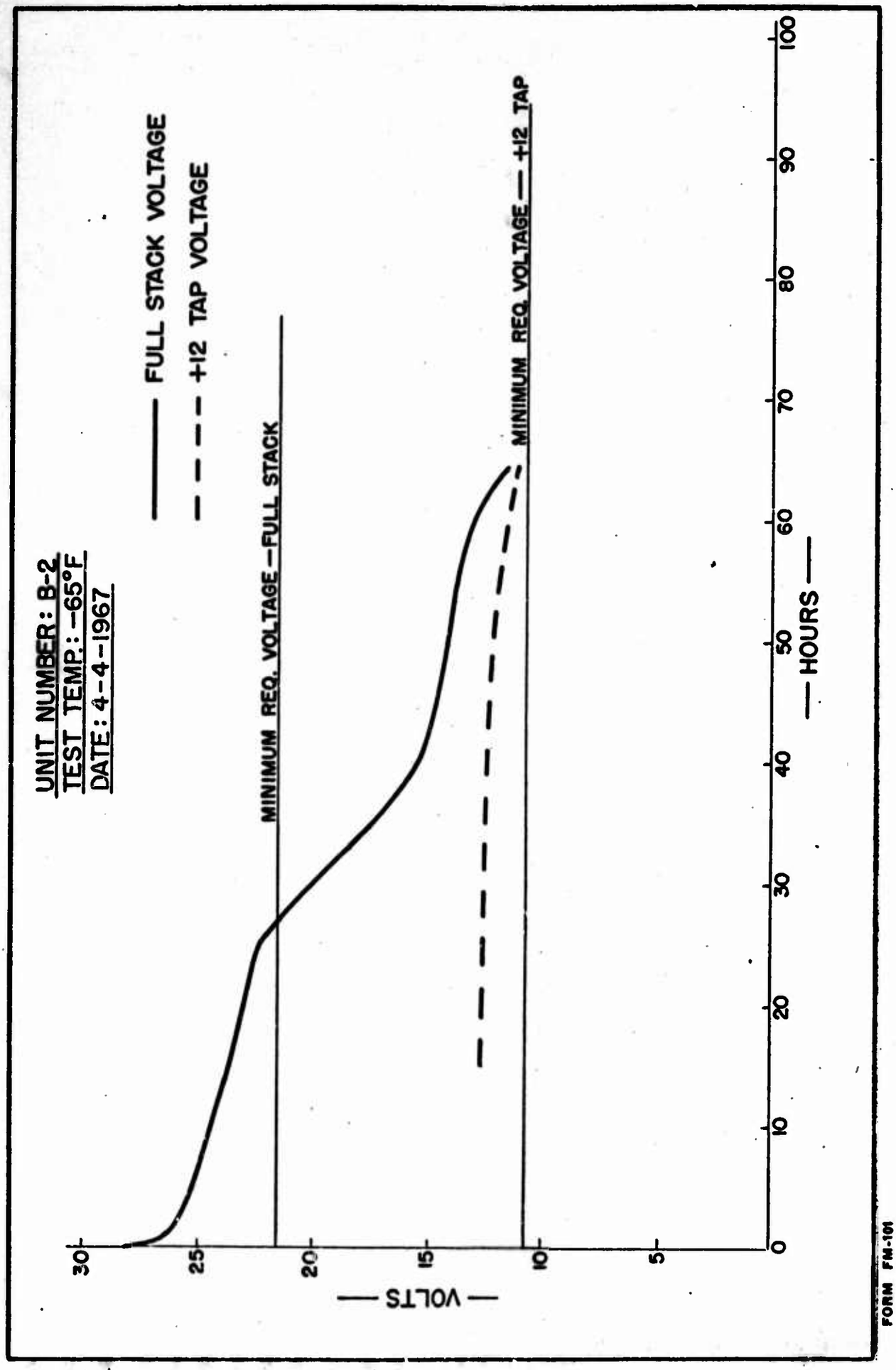

Figure R

Partial Test Interpretation

(U) 11.4 Discharge curves for tests of Units 13G, 10G, and 11G are presented in Figure S, showing total voltage behavior over the 50-hour discharge period. Pulse voltages are shown for 24-volt and 12-volt levels in Figures T, U, and V at low, high, and ambient temperature test environments. Further test performance detail is shown by individual voltage tap for both standby and operate conditions in Figures W, X, and Y, again at specified environmental temperature levels.

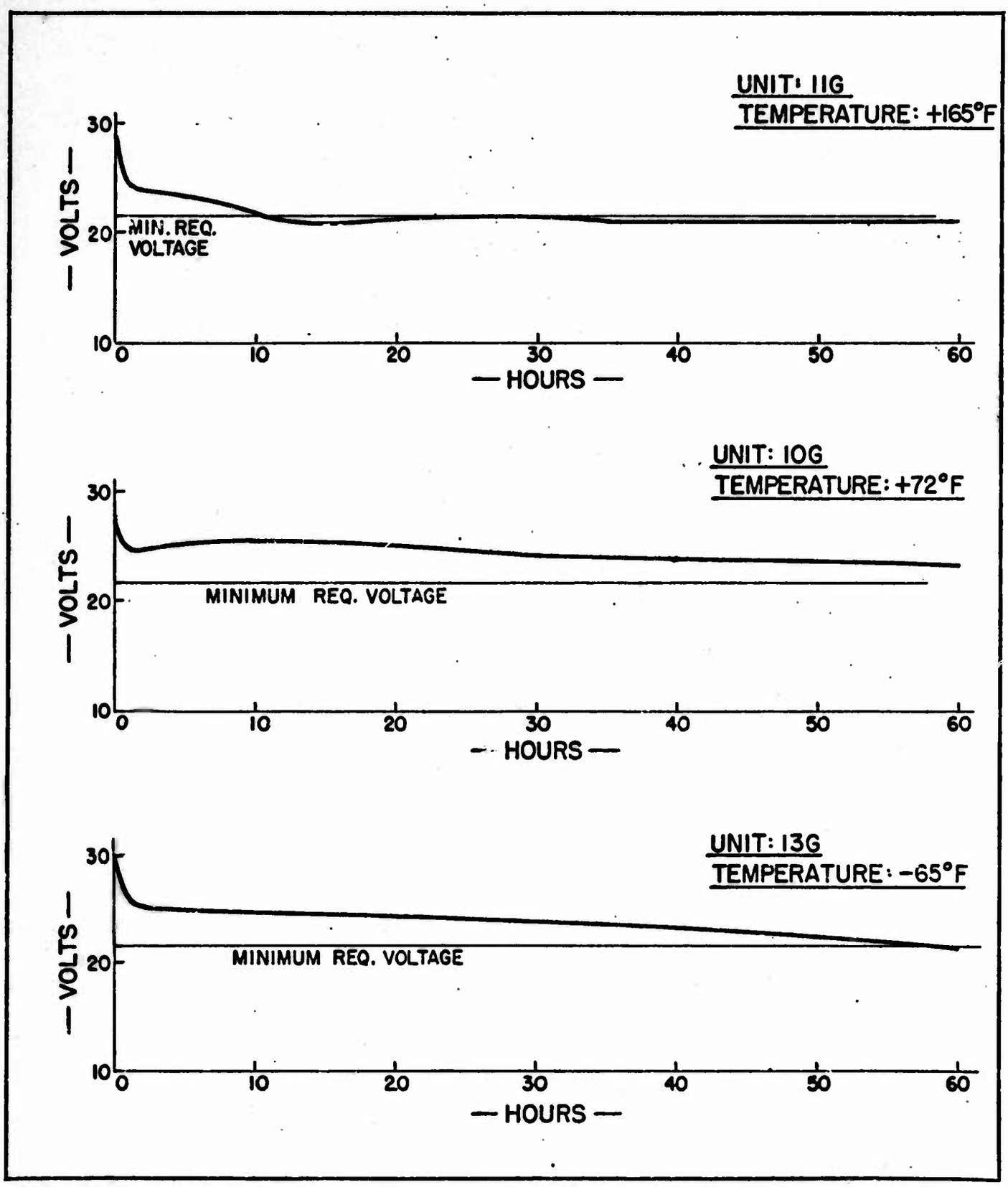

FORM FM-100

Figure S

Final Performance Curves

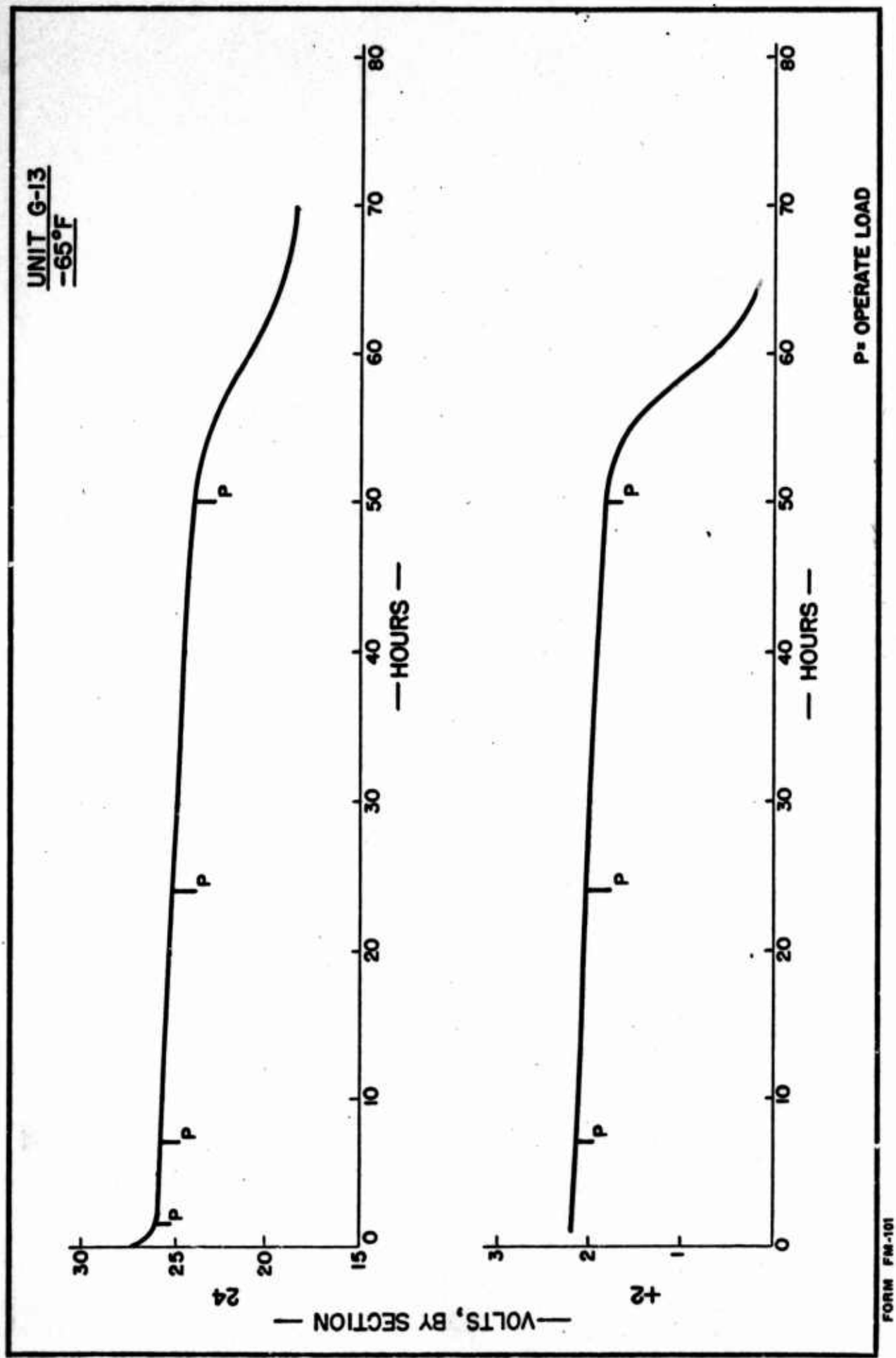

Figure T

Final Performance Curves

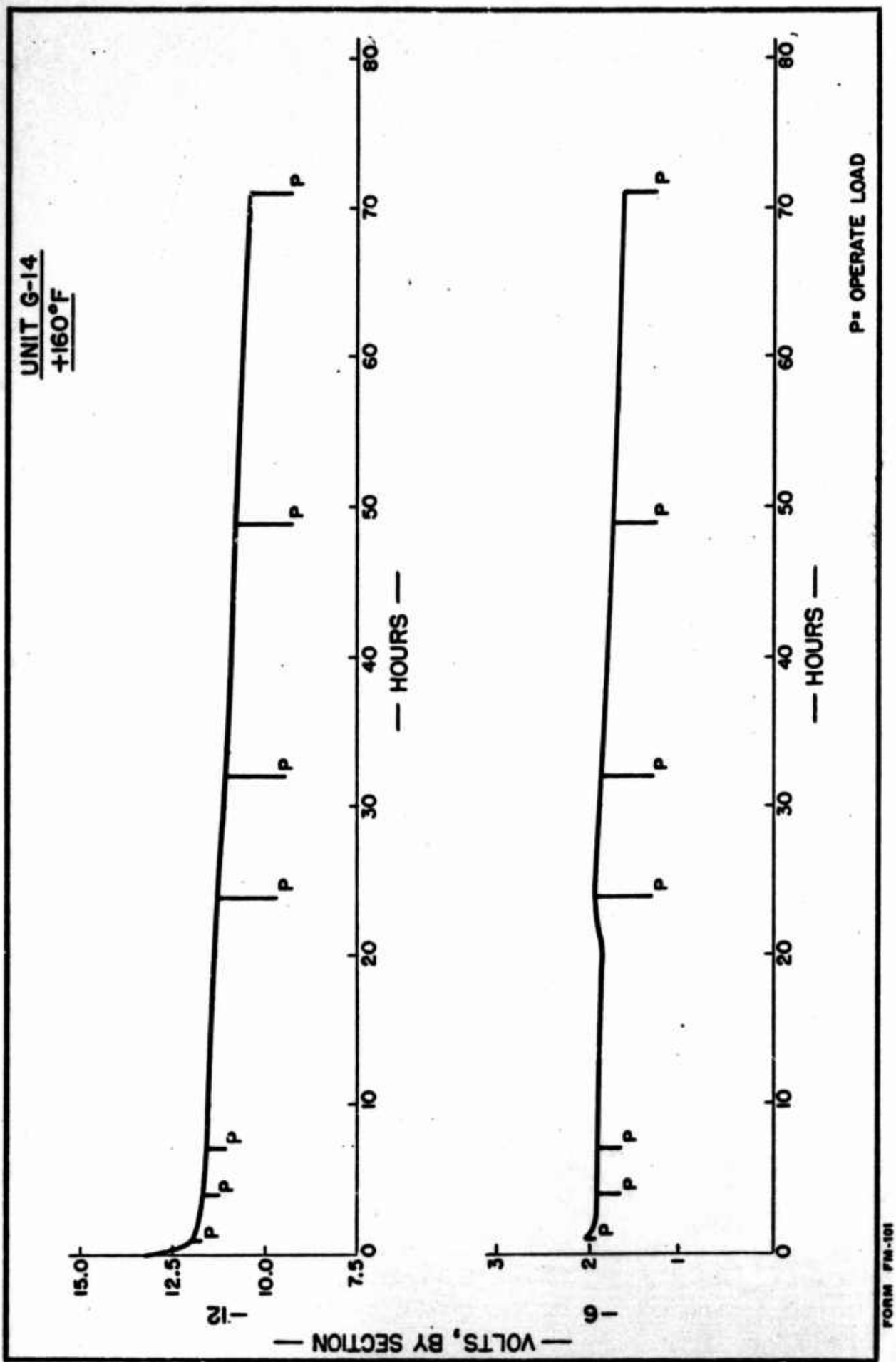

Figure U

Final Performance Curves

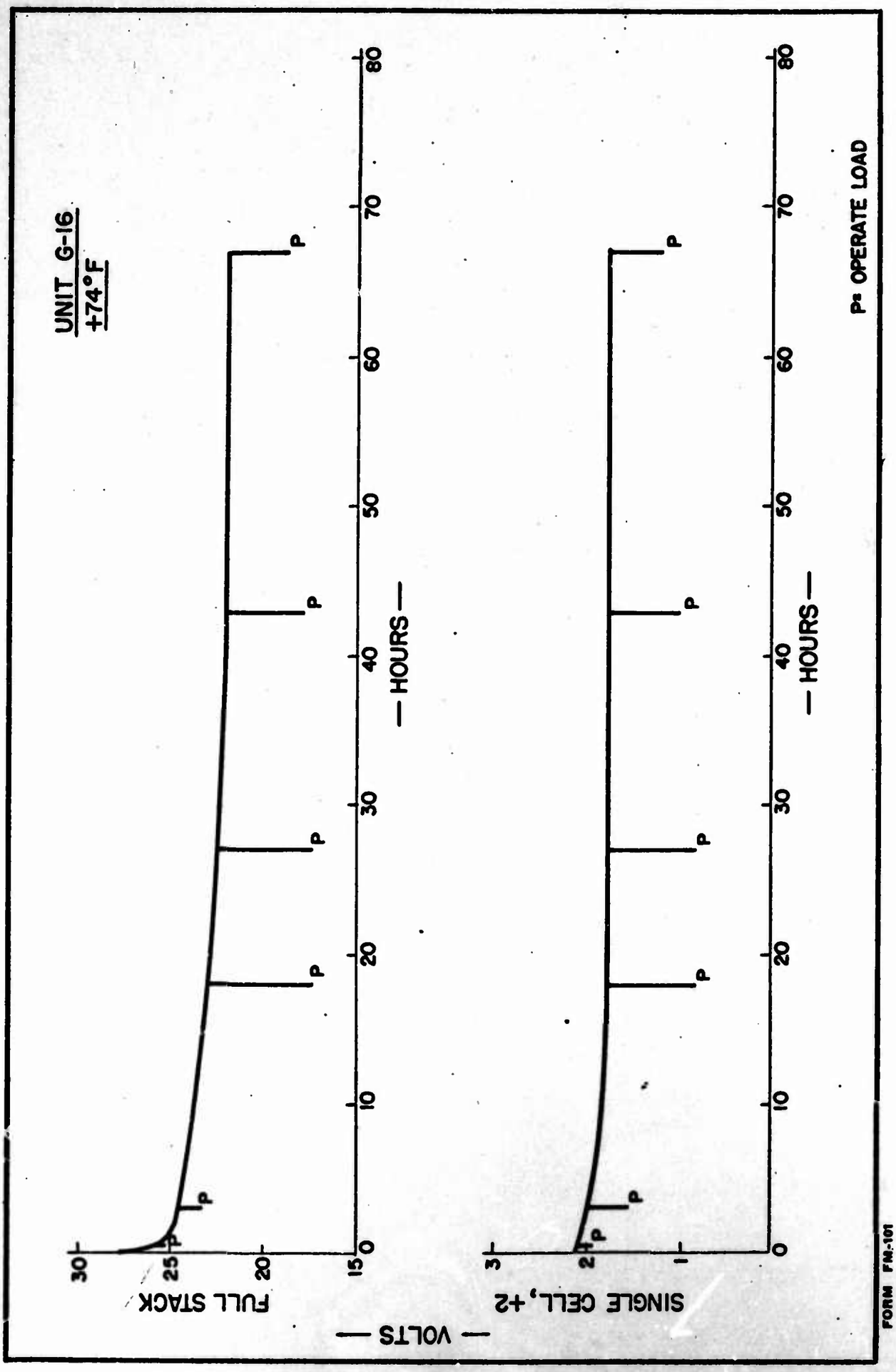

Figure V

Final Performance Curves

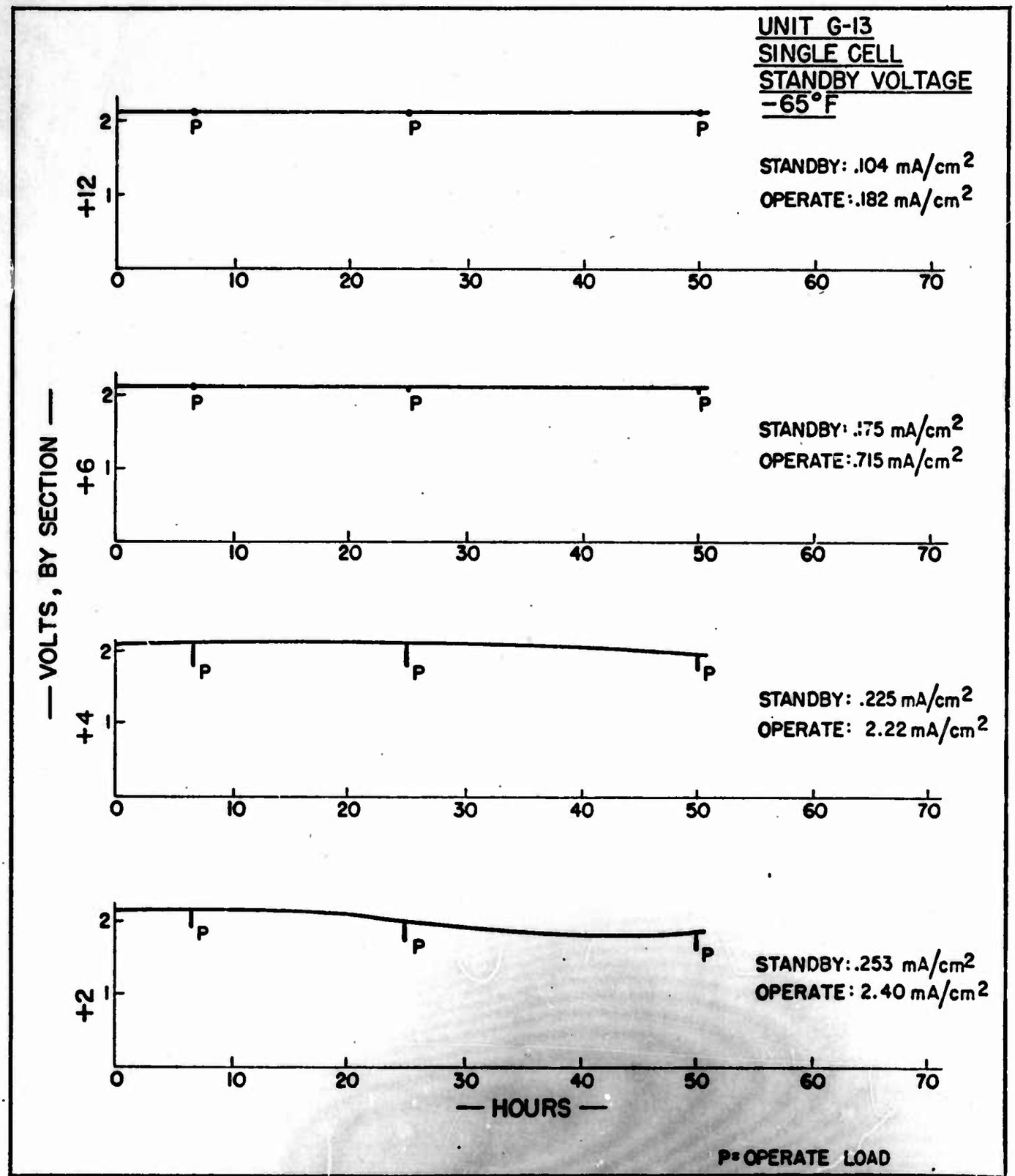

FORM FM-100

Figure W

Final Performance Curves

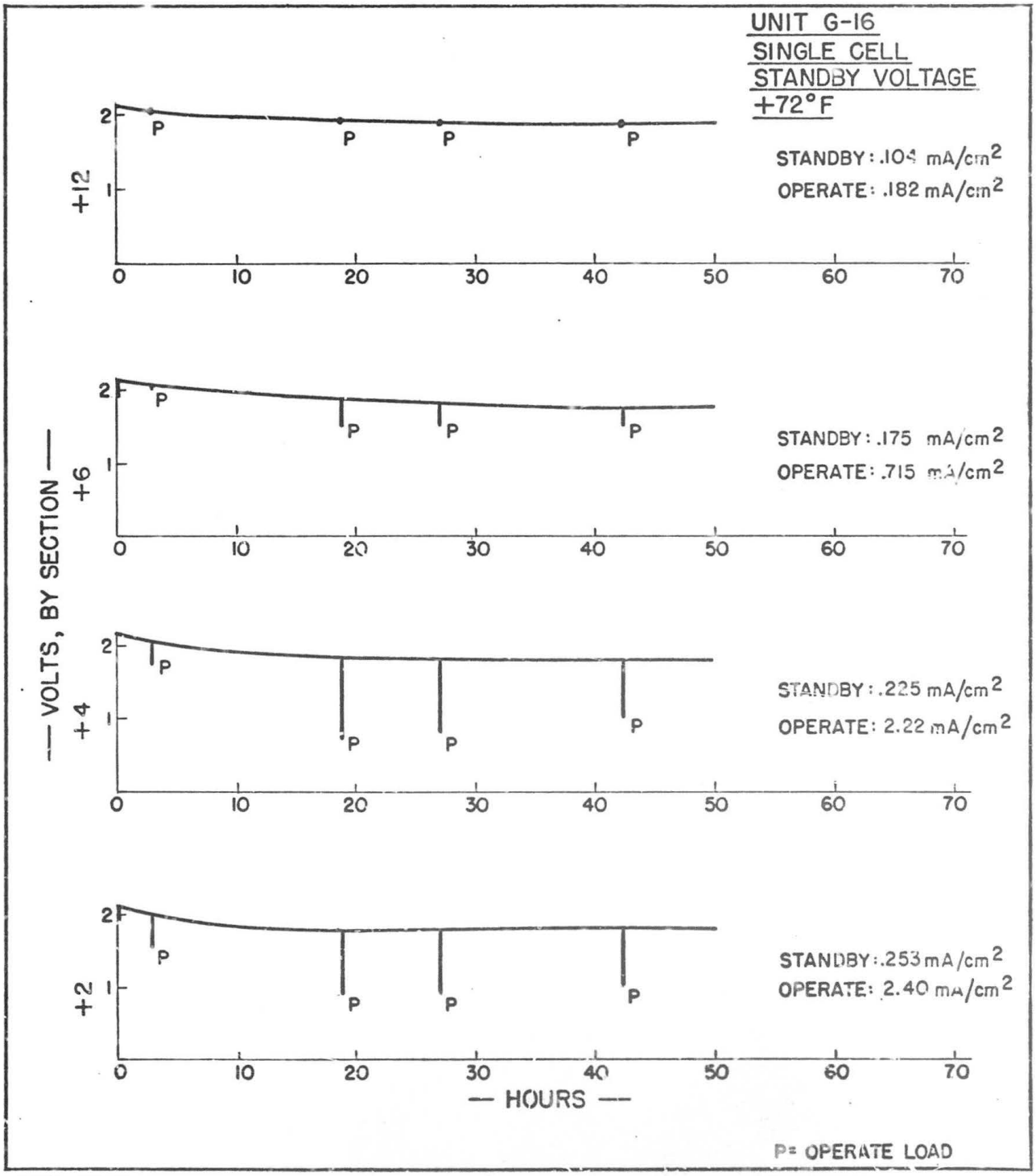

FORM FM-100

Figure X

Final Performance Curves

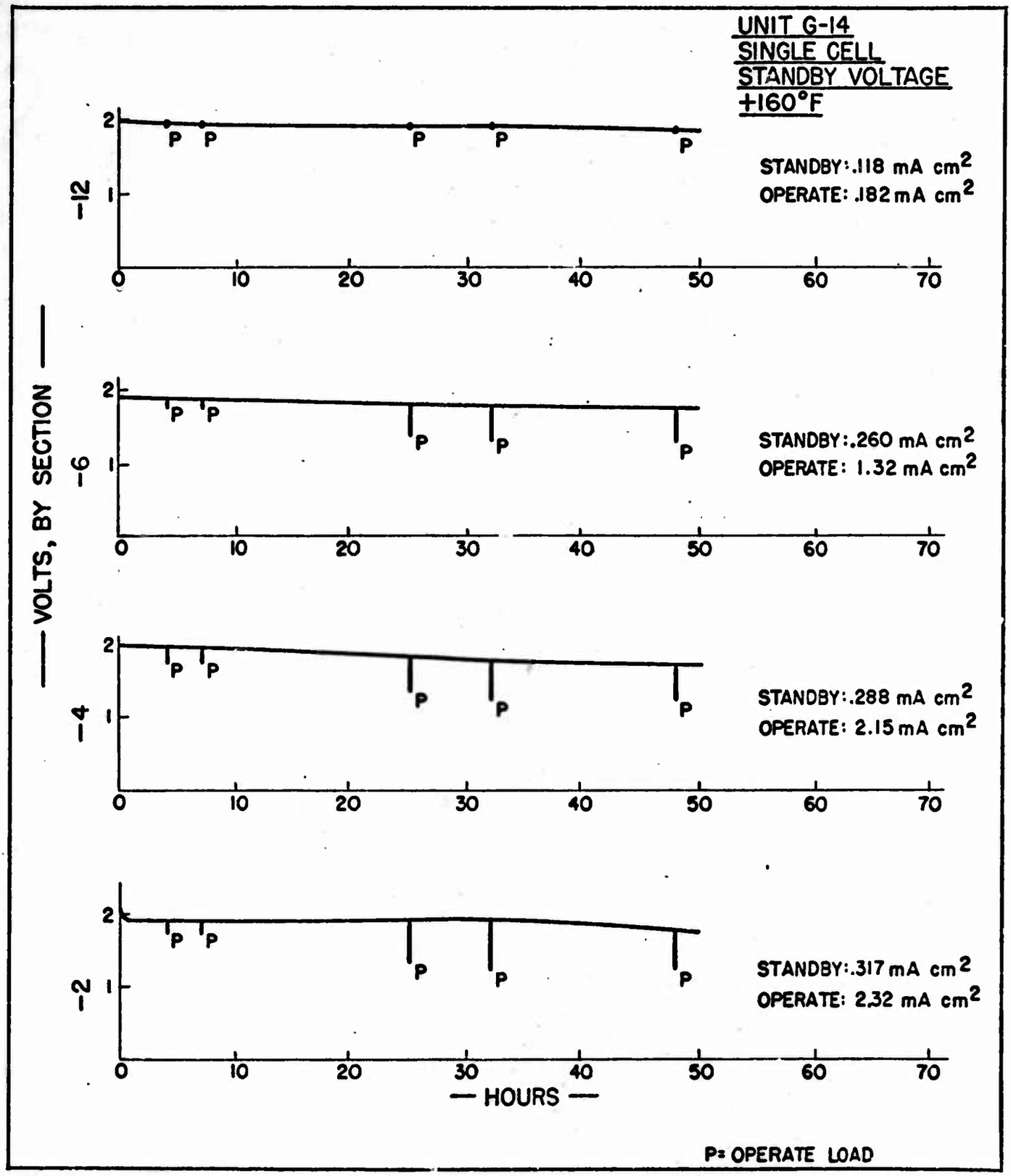

FORM FM-100

Figure Y

Final Performance Curves

12.0 Heating Effects (U)

(U) 12.1 Considerable attention has been given to the heating effects produced by the battery. Although the reactions involved are not highly exothermic, some heat is produced, and this tends to extend the operating temperature beyond the +165°F upper limit. Because the battery is intended for end use in a closed container, it was felt that other components in close proximity might be affected by such heating.

(U) 12.2 A special study on the causes and effects of battery heating was conducted and reported separately. Such effort is covered as Appendix I to this summary.

(U) 12.3 Final testing of battery units was done with the battery actually mounted in weapon fixtures. Thermocouples were located at various surfaces to observe dissipation of heat. Peak temperatures were observed to be in the +195°F to +200°F range after approximately three hours of discharge, tapering off for the balance of the operating period. Control surface monitor showed peak excursion to approximately +170°F, well within the range considered safe to components. Figure Z shows placement of temperature sensing units and typical results obtained.

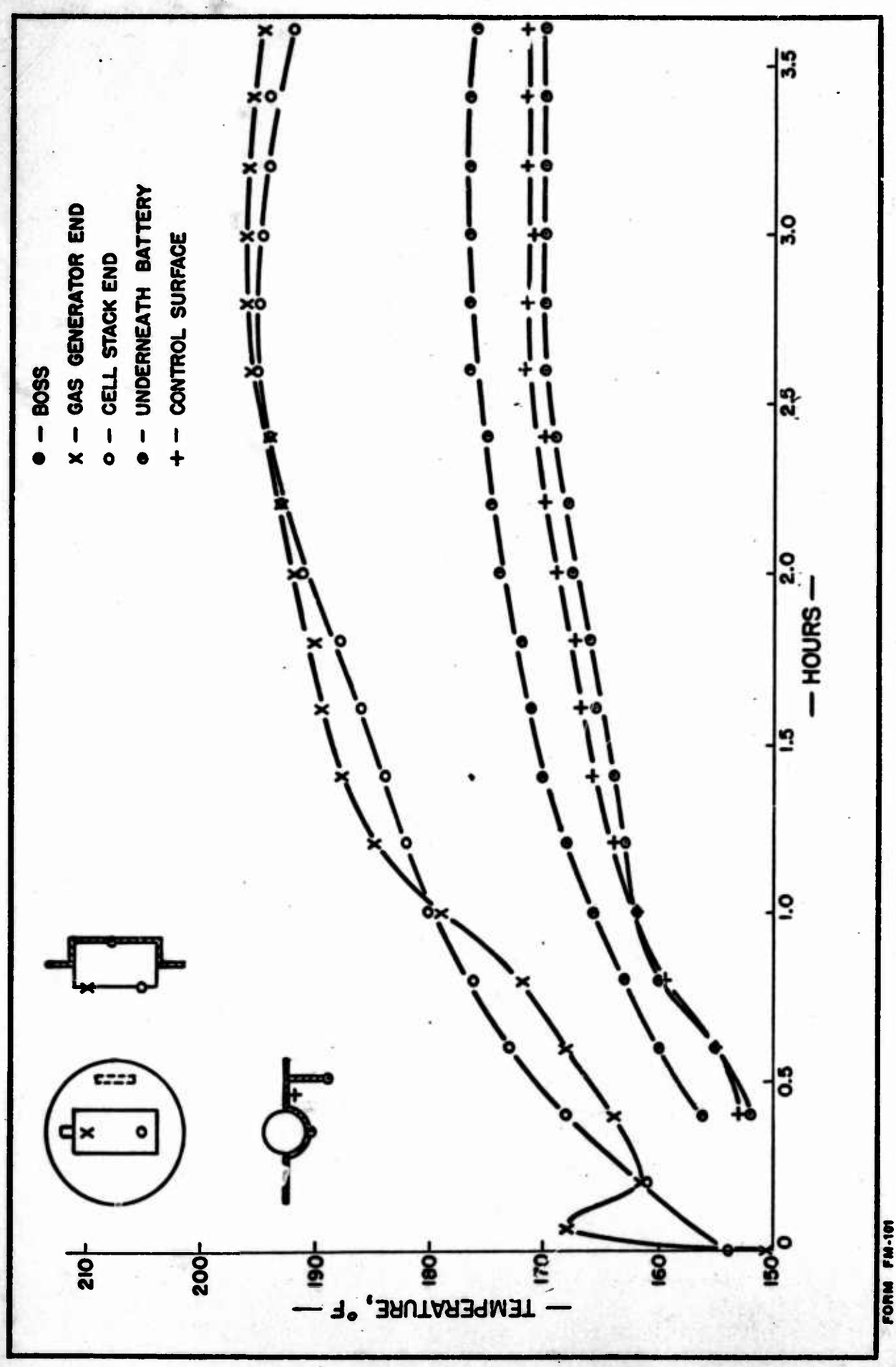

Figure Z

Temperature Monitor Curves

13.0 Distribution (U)

	Copies
Commanding Officer Picatinny Arsenal Dover, New Jersey 07801 Attention: SMUPA-PB1	8
Commanding General Army Materiel Command Washington 25, D. C. Attention: AMCRD-DE-N	1
Armed Services Technical Information Agency Defense Documentation Center Cameron Station Alexandria, Virginia 22314	10

Appendix I

SPECIAL ENGINEERING STUDY

HEATING EFFECTS IN THE 625-A

AMMONIA BATTERY DESIGN

TABLE OF CONTENTS

Engineering Study Covering Heating Effects in the 625-A Ammonia Battery Design

I. Introduction

Throughout the course of developmental testing it has been observed that batteries of the 625-A design display a temperature rise upon activation or during discharge. Since this phenomenon was to a certain extent peculiar to this particular application of liquid ammonia electrochemistry (i.e., other battery designs using similar electrochemical concepts displayed much less pronounced evidence of heating), it was felt that heating might somehow be correlated to satisfactory performance or more specifically to the lack of satisfactory performance.

Additional concern prompting this study was the need to relate potential heating effects of the battery with respect to other components situated in close proximity in the end device. Although previous observations of heating had been recorded, no direct analysis was made until this study. This is principally because heating was judged to be caused by improper design function which has been experienced far beyond normal expectations in the 625 design.

II. Objective

The primary objectives of this study were to determine the cause or causes of battery heating, and to provide sufficient data to allow projection of heating effects to be anticipated in the final battery package.

III. Summary

Because of the very high cost of testing prototype 625-A batteries in large quantities and the lack of adequate control data, a smaller but similar battery construction was used as a test vehicle. A series of tests were conducted monitoring temperature rise in as completely controlled an environment as was possible to construct. Quantitative data of such comparable units was obtained for batteries under varied loading conditions, varied exothermic reaction producing material and varied degrees of controlled internal electrical leakage. Thermal gradients were then studied as a function of time and battery discharge performance against control units.

Results obtained showed principal causes of battery heating to be (1) rate of reaction, (2) quantity and reactivity of electrolyte salts and (3) internal electrical leakage between cells. It has been established that battery heating can be minimized but not eliminated

from the design and that heating effects generally relate in an inverse manner to satisfactory levels of performance in the intended application.

IV. Procedure

A test vehicle having proportional chemical composition and similar mass relationships to the 625-A battery design was fabricated. These units (modified G2492 battery assembly) were constructed in as nearly identical fashion as possible under laboratory conditions. Variables selected for examination were scheduled to be significantly above and below levels normally utilized in the 625-A design.

All units were tested using identically calibrated monitoring devices in a specially constructed test environment in a fashion similar to calorimetric determinations. The prime index of evaluation used was temperature change as a function of battery activation and discharge, this being continuously traced on recording equipment by precisely controlled thermocouple locations. Figure I represents pictorially the test setup. All temperature data were recorded on one multichannel Honeywell Electronik instrument. Battery output voltage was monitored on a Rustrak Model 88 recorder. Battery loads were made up of low tolerance decade resistances and verified before each test.

Three control tests were run initially to obtain qualification of equipment, test setup and an acceptable index of test reproducibility. Two percent accuracy was considered an acceptable margin of validity.

V. Test Plan and Observations

A. Variation in Loading

The first three tests were run with the following results. In these units all construction and content were proportional to the 625-A design. The rate of reaction was varied at three levels from no load (open circuit), to a load equivalent to the intended design (900 ohms), to twice the anticipated design rate (450 ohms).

it No.	Load (ohms)	Useful Life Hours	Peak Voltage	Peak Temp.	Peak Occurrence Hours	Relative Heat Generated*
1843	No Load	118+	10.9	136°F	3.0	0.83
1913	900	67.5	10.9	139°F	3.0	1.00
1973	450	41.5	10.8	140°F	3.0	1.08

alculated at 15 hours after activation.

Analysis

Based on the preceding three tests it can be illustrated that heating effects of ammonia batteries are proportionally related to the rate (current) of the electrochemical reaction. Relationships as established in Figure II were assumed for the given active surface reaction. Using the available anode surface area, it is then convenient to translate heating effects as being proportional to current per square unit of active cell surface.

Because the resistive load selected for Unit #1913 (900 ohms) was calculated as equivalent to current per square unit of anode surface found in the proposed 625-A design, the relationships are held to be, likewise, true. This would indicate that heating effects present in the design could be controlled by reducing or increasing the load to the extent shown by the relative index of temperature rise.

The present design is indicated as being relatively well-optimized for the current producing requirement as shown by the fact that doubling the load increases heating effects by a factor of only 0.08.

As might be expected, the useful discharge life to any arbitrary cutoff voltage was inversely proportional to current drain and at the design value (900 ohms) did yield life commensurate with that experienced in 625-A prototypes.

B. Salt Content

The second test series utilized identical test units except for variation in salt content. Because various salts are included in different portions of the cell design, the following test levels were established.

Test No.	Content
10287	Double anolyte salt content/normal catholyte*
10281	No anolyte salt content/normal catholyte
10288	Normal anolyte salt content/no catholyte salt
10283**	Double anolyte salt content/normal catholyte
10282	No salt content/no salt content

* Normal used to indicate equivalent to 625-A design.
** No load.

Based on previous experience, the two types of salts utilized in ammonia battery chemical design are selected with respect to conductivity. The more chemically active acid salts have been found to be operationally satisfactory when employed singly, however, excessive quantities are normally required to provide proper conductivity levels. Likewise, both anolyte and catholyte salts have previously been determined to exhibit characteristic heating effects upon solution in NH_3. For this reason, the preceding test schedule was selected to examine the extremes.

Heat of ammoniation which represents a physical property of salt compounds is expected to reflect some temperature rise upon initial battery activation. Proper design schedules which utilize corresponding endothermic characteristics of NH_3 being released from storage into a relative vacuum (cell chamber is maintained at one atmosphere in storage) show a degree of compensatory thermal effects. In any case, heat generated and subsequent temperature rise are associated characteristically with the early portions of the discharge period and are dissipated relative to the surrounding environments. In this test fixture, insulation was considered sufficiently effective to sustain the period of initial heating for longer periods of time than found in actual item usage.

Results obtained were as follows:

Unit No.	Load (ohms)	Useful Life Hours	Peak Voltage	Peak Temp.	Peak Occurrence Hours	Relative Heat Generated*
10287	900	84	11.2	143°F	3.0	1.06
10281	900	59	10.7	134°F	2.0	0.92
10288	900	15	10.8	104°F	3.0	0.45
10283	No Load	116+	11.2	144°F	3.0	1.04
10282	900	None	5.1	93°F	2.0	0.21

* Calculated at 15 hours after activation.

Analysis

Results indicate that contributive effects to battery heating from the salt content overshadow, at least for the initial periods of discharge, other potential sources of heat. As might be expected, the test which utilized only catholyte salt (Unit #10281) reached a peak temperature earlier than other combinations. This is felt

to be because the catholyte salt is more active chemically than the relatively neutral anolyte salt. Because the unit had no anolyte salt and only the normally scheduled quantity of catholyte salt, useful life could be expected to be reduced. This was borne out (59 hours) and was complimented by the fact that the inverse condition (Unit #10288 with no catholyte salt) also ran for a reduced period (15 hours) showing significantly less heating (104°F peak).

A review of performance in terms of discharge illustrates that period of active life is significantly affected when salt contents are manipulated. Best discharge time was replicated from the first test series (No Load #10283) but with highest observed heating effects. Poorest performance, quite expectedly, was observed with no salt content and greatly reduced heating.

In order of contribution to heating effects observed in this series the catholyte salt is the largest source of heat, the anolyte salt the second largest source, and possible interactive effects of salt content and loading appear minimal. Complete withdrawal of all salt content is represented by small, but observable, heat sources.

C. Anode and Cathode Contributions

The only remaining sources of heat in the cell design are by subtraction identified with the anode or cathode; these being the only remaining component materials. The next test series attempted to evaluate the contributive heat effect of each.

Test No.	Description
10272	Utilization of alternate oxidant of an insoluble nature for a cathode material. Quantity regulated to be of an equivalent electrochemical capacity.
10065	Complete absence of anode material.

These tests yielded the following results:

nit No.	Load (ohms)	Useful Life Hours	Peak Voltage	Peak Temp.	Peak Occurrence Hours	Relative Heat Generated
0272	900	27	10.8	99°F	4.0	0.45
0065	900	None	1.4	99°F	0.2	0.12

Analysis

The data from this series of tests indicates that contributive effects of the anode to cell heating are relatively negligible. Observed heating effects due to solubility of the design cathode oxidant are significant although the peak occurrence does not happen at the same point in discharge as does the effect of previously examined variables.

In terms of performance, the less soluble cathode material does not yield sufficient reaction behavior to meet the requirements of this design. The absence of anode material, of course, does not yield useful discharge at all.

It is interesting to note that in the process of establishing the 625-A design, a large number of alternate cathode materials known to be compatible with ammonia battery chemistry through previous independent development were examined. None were found to be as satisfactory for the 625-A application as the organic oxidant (metadinitrobenzene) presently being used. All feasibility estimates were based upon the utilization of this material.

D. Intercell Electrical Leakage

Because the 625-A design calls for the utilization of many series-connected cells to establish the required operational voltage, and because these cells are subjected to a common conductive electrolyte, energy dissipated as heat from electrical leakage cannot be ignored.

A test situation to compare the relative contribution to battery heating effects from this source was established by specially constructing batteries with all cells wired in parallel rather than series. Maintenance of the same cell potential than allows consideration of temperature rise without intercell leakage effects.

Results from two specially constructed batteries were as tabulated:

nit No.	Load (ohms)	Useful Life Hours	Peak Voltage	Peak Temp.	Peak Occurrence Hours	Relative Heat Generated
0277	180	94+	2.31	129°F	2.0	0.90
0278	180	94+	2.31	130°F	2.0	0.92

Analysis

Data yielded by the described treatment for elimination of intercellular leakage effect shows a heating characteristic which is less than that obtained in normal series cell arrangement. This would indicate that some heat is contributed by intercell leakage and although not verified by this examination, it is logical to assume that such intercell leakage would be directly proportional to the number of cells in a common electrolyte situation.

In all tests conducted for purposes of this study, five cells were used. Content and hardware mass relationships were proportionally reduced to be equivalent to a five-cell 625-A battery. The 625-A design application requires the use of 12 cells in series and it is reasoned that heating due to intercell leakage could logically be estimated in a direct 5 to 12 increase relationship; all other factors being the same by virtue of the test model.

E. Gas Generator Heat Contribution

All battery units used in this test were initiated with similar gas generating devices. Physical design and the unique characteristics of these pyrotechnic devices prevented a uniform scaling factor from being employed which was commensurate with other design parameters.

Actual 625-A batteries have been tested with special monitoring precautions to record effects of gas generator heat contribution. For purposes of this study, it was assumed that because identical units were employed, contributive heat generated by the gas generator device would be constant and thereby available through a common factor not affecting other determinations.

VI. Series Analysis and Conclusions

By comparison of a relative temperature rise index based on the initial control units as displaying a composite of all heating effects, it can be observed that almost all factors examined have some contributing effect to battery heating. Factors having the least effect are anolyte salt and cell loading while those having the greatest effect are catholyte salt content, intercell leakage and cathode reaction. Inasmuch as heating effects were observed when critical elements of the cells were missing, i.e., salt and anode materials, it can be concluded that gas generator heat transfer does play a minor part in the total derivation of heat, as well as other factors not identified in this study.

A comparison of performance data, overall, would indicate that although some reduction of heating effects may be possible through manipulation of heat sources present in the design, a corresponding reduction in performance is probable if major shifts are endeavored.

The fact that discharge performance recorded in hours frequently exhibits better than required durations, can be accommodated by the nature of the reduced scale batteries used for this study. Intercellular leakage in addition to being a logical source of heat, likewise, dissipates useful energy producing material on a 12/5 ratio as well. Likewise, the models employed were physically smaller which has the effect of decreasing inefficiencies found in the full size design through material availability, i.e., larger parts structures.

Because of the nature of heat sources identified in this study, it can be concluded that significant battery heating is present in a defined time of operation. In all observed cases operating temperatures of batteries have shown a steady decrease after the occurrence of a peak temperature in the first two to three hours of operation.

In an attempt to project, from these and other data, a characteristic behavior of the end design item it is considered practical to observe that heat produced within the battery has a distinctly troublesome effect upon package design by virtue of the increased pressures reflected by the electrolyte. This phenomenon is regenerative in nature, in that failure of package allows more heating which causes further package destruction. This is particularly true at high temperature environments.

Assuming that mechanical breakdown of package can be prevented from initiating a destructive heat buildup cycle by means of appropriate quality control measures, it is then reasonable to interpret temperature rise inherent in the battery design with the quantitative data presented in Figures III through XIII which show battery temperature compared to environment.

Using control Test #1913 as representative of proper function as presently designed (Figure IV) a temperature rise of 57°F is observed over a period of three hours decreasing to less than 10°F above the environment at 18 hours. In the present design requirement extreme this would equate to a peak skin temperature of 217°F (160 + 57) if operation similar to Test #1913 were to be obtained. Assuming less perfect insulation than present in the laboratory test situation, it is probable that a less prolonged period of heat retention would be present.

To minimize heating effects the following directions for design movement are indicated as positive.

(1) Minimize catholyte salt content.

(2) Minimize internal electrical leakage.

(3) Compromise high temperature environment.

(4) Utilize a less soluble oxidant material.

(5) Reduce current density of the battery package.

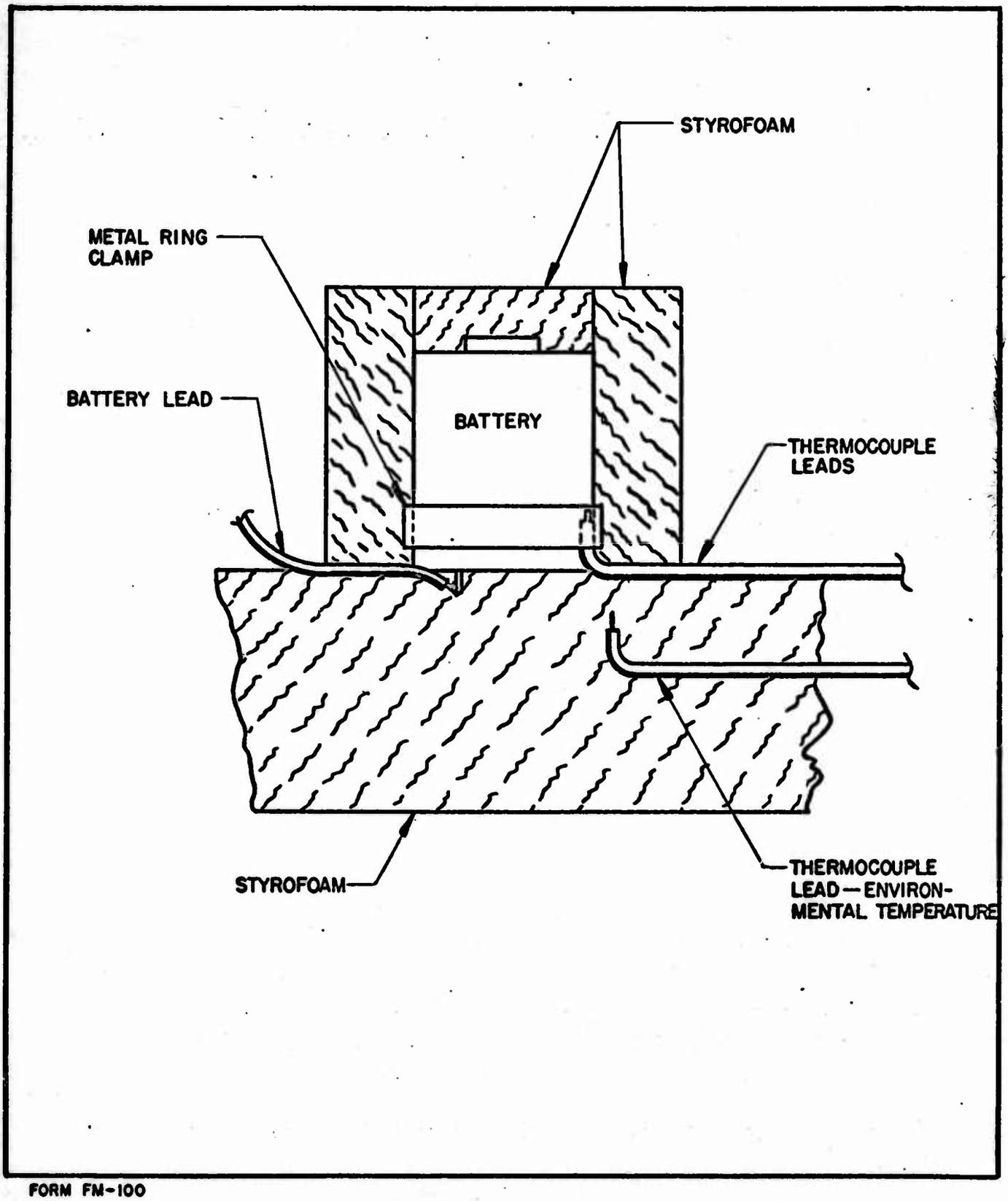

FORM FM-100

FIGURE I

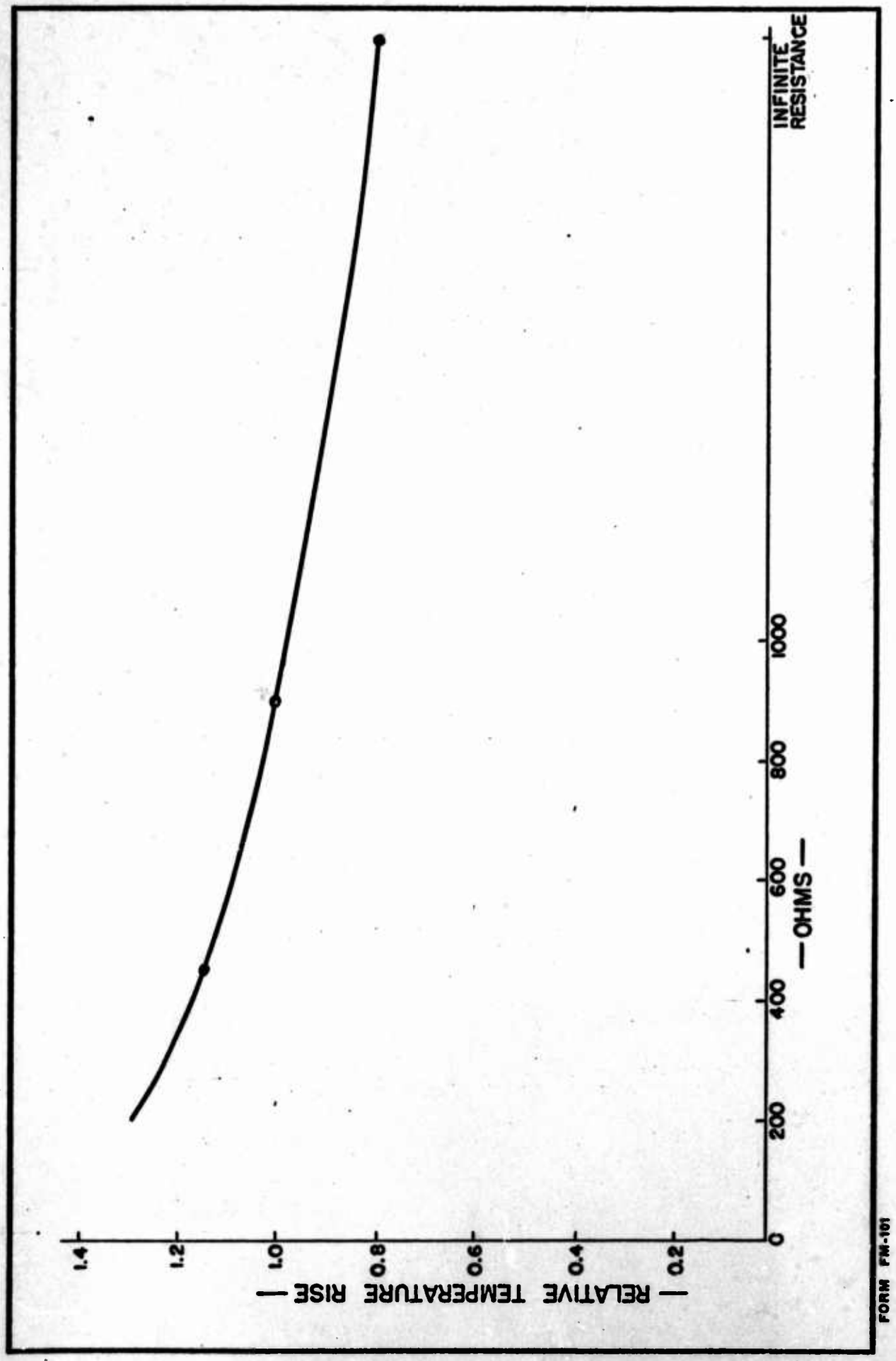
RELATIVE TEMPERATURE RISE
1.4
1.2
1.0
0.8
0.6
0.4
0.2
0
200
400
600
800
1000
INFINITE RESISTANCE
OHMS
FORM FM-101

FIGURE II

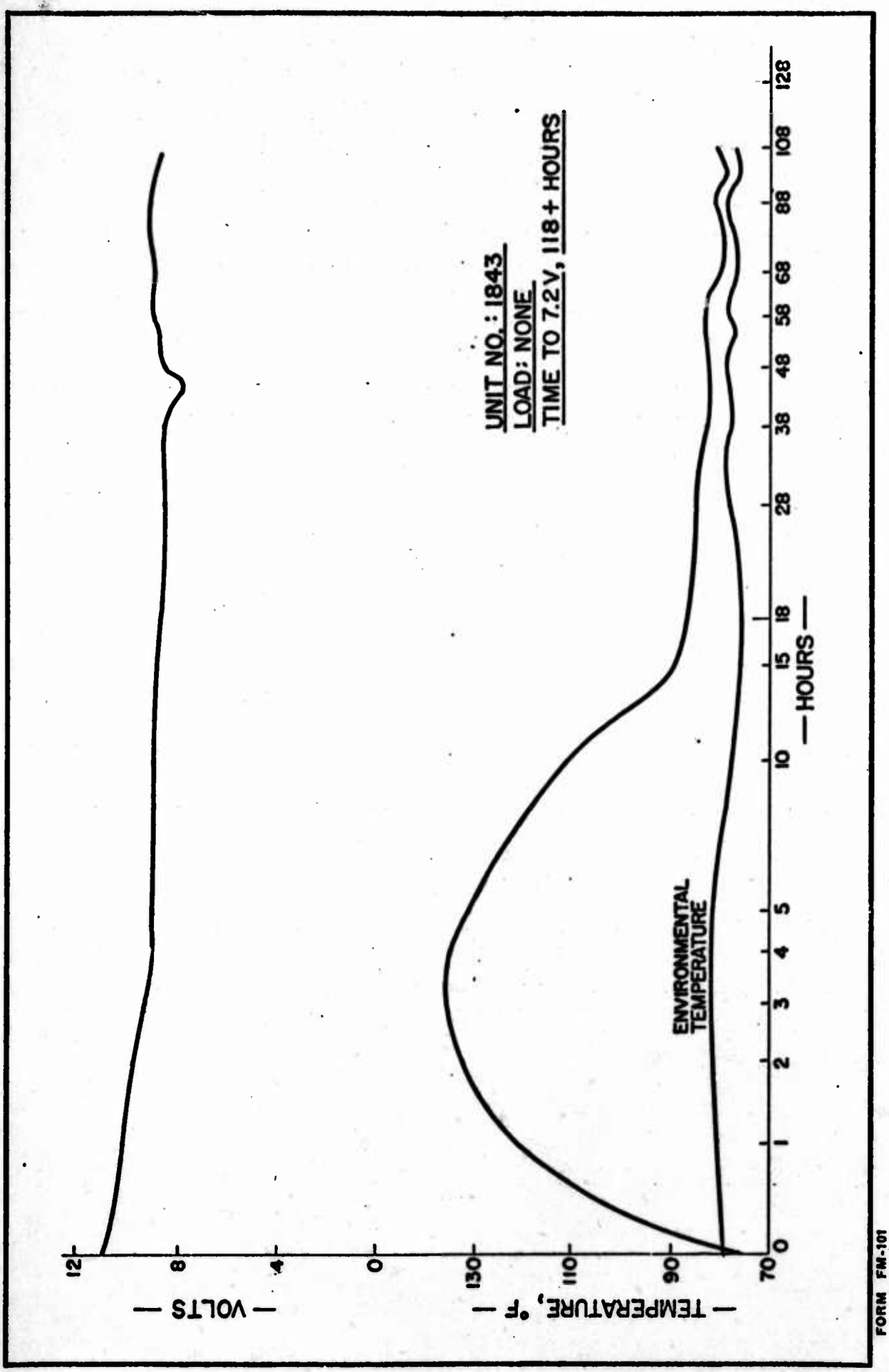
UNIT NO.: 1843
LOAD: NONE
TIME TO 7.2V, 118+ HOURS
ENVIRONMENTAL TEMPERATURE
— VOLTS —
— TEMPERATURE, °F —
— HOURS —
12
8
4
0
130
110
90
70
0
1
2
3
4
5
10
15
18
28
38
48
58
68
88
108
128
FORM FM-101

FIGURE III

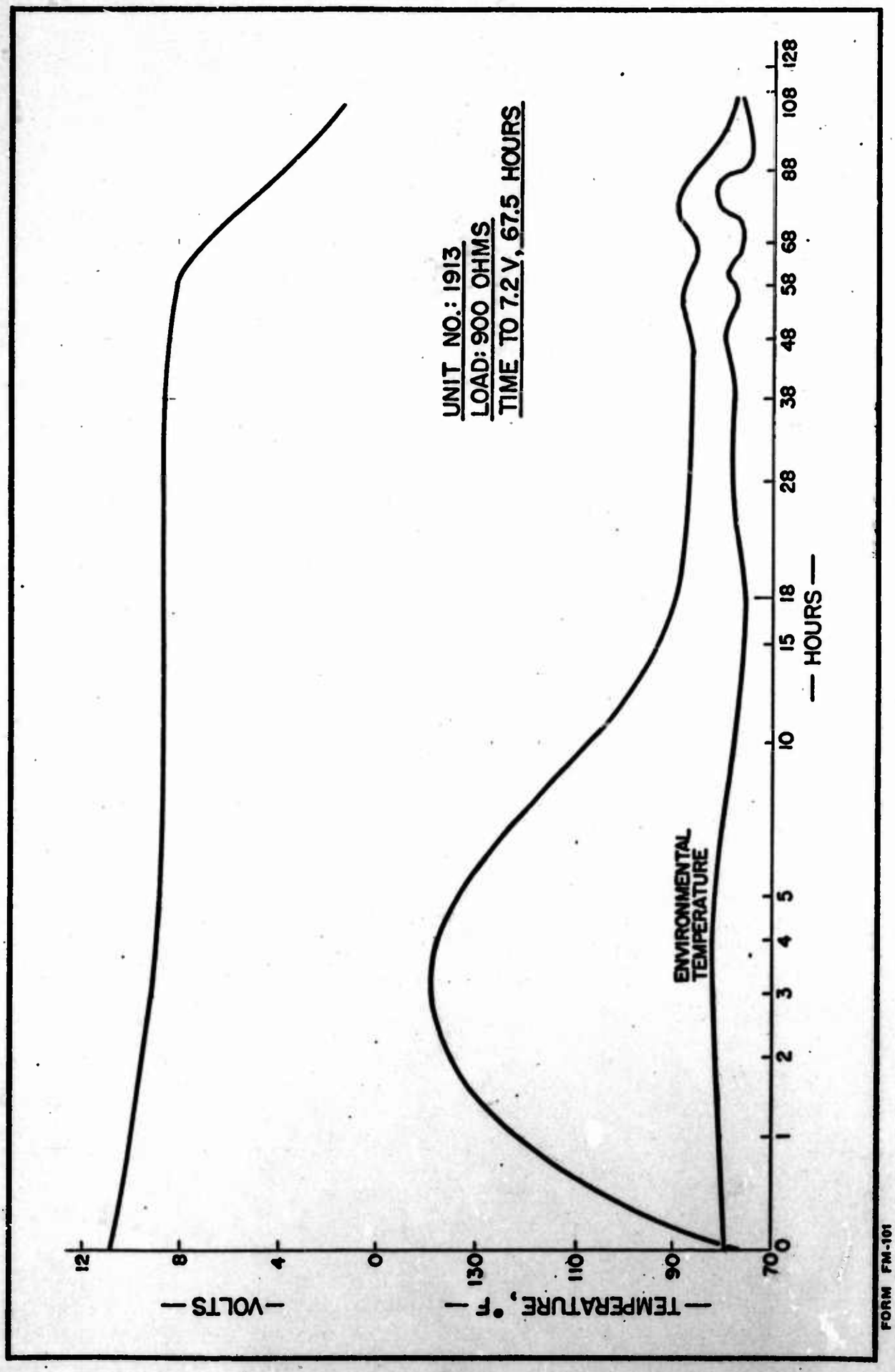
UNIT NO.: 1913
LOAD: 900 OHMS
TIME TO 7.2 V, 67.5 HOURS
— VOLTS —
12
8
4
0
— TEMPERATURE, °F —
130
110
90
70
ENVIRONMENTAL TEMPERATURE
0
1
2
3
4
5
10
15
18
28
38
48
58
68
88
108
128
— HOURS —
FORM FM-101

FIGURE IV

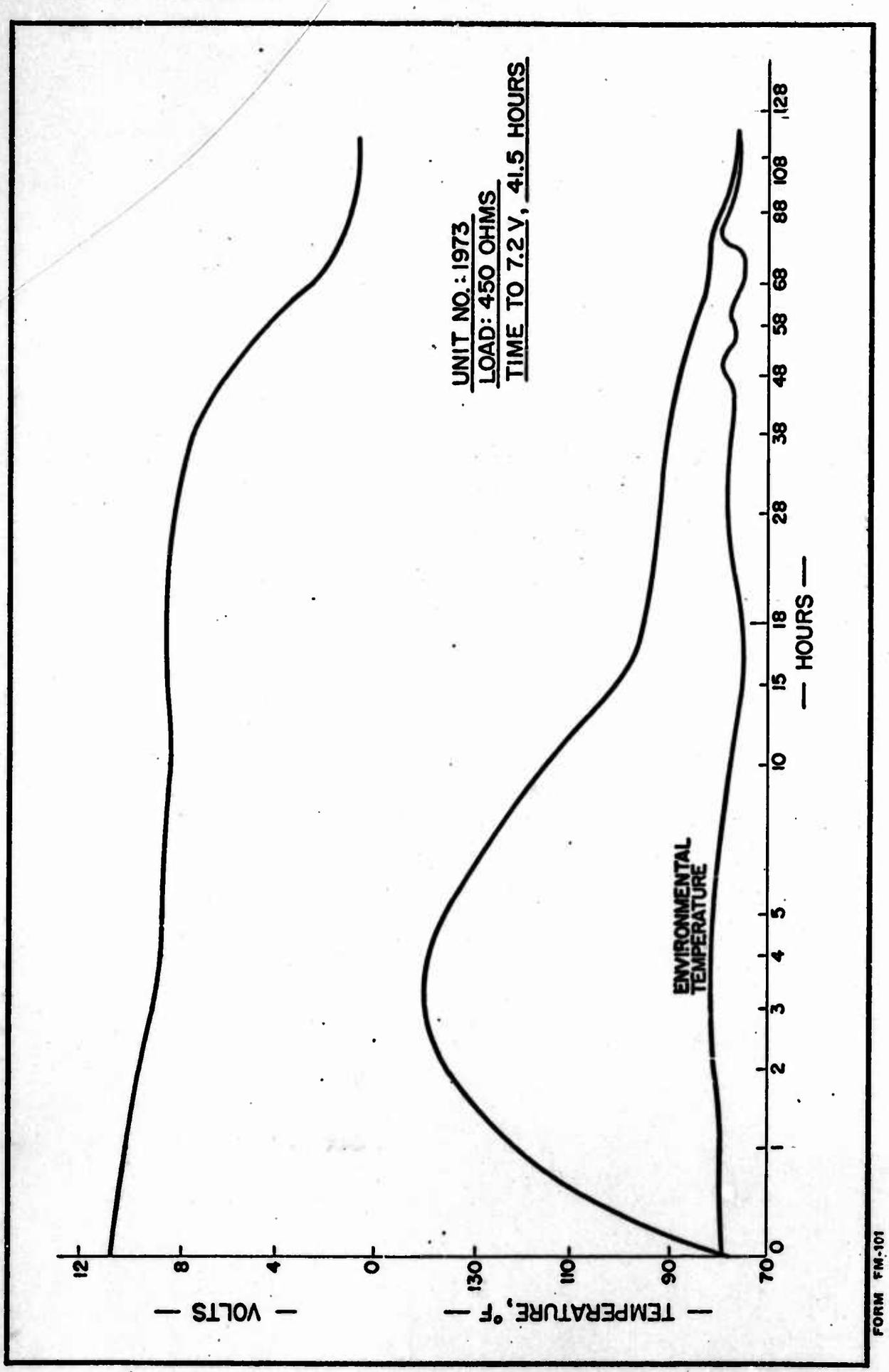
UNIT NO.: 1973
LOAD: 450 OHMS
TIME TO 7.2 V, 41.5 HOURS
— VOLTS —
12
8
4
0
— TEMPERATURE, °F —
130
110
90
70
ENVIRONMENTAL TEMPERATURE
0
1
2
3
4
5
10
15
18
28
38
48
58
68
88
108
128
— HOURS —
FORM FM-101

FIGURE V

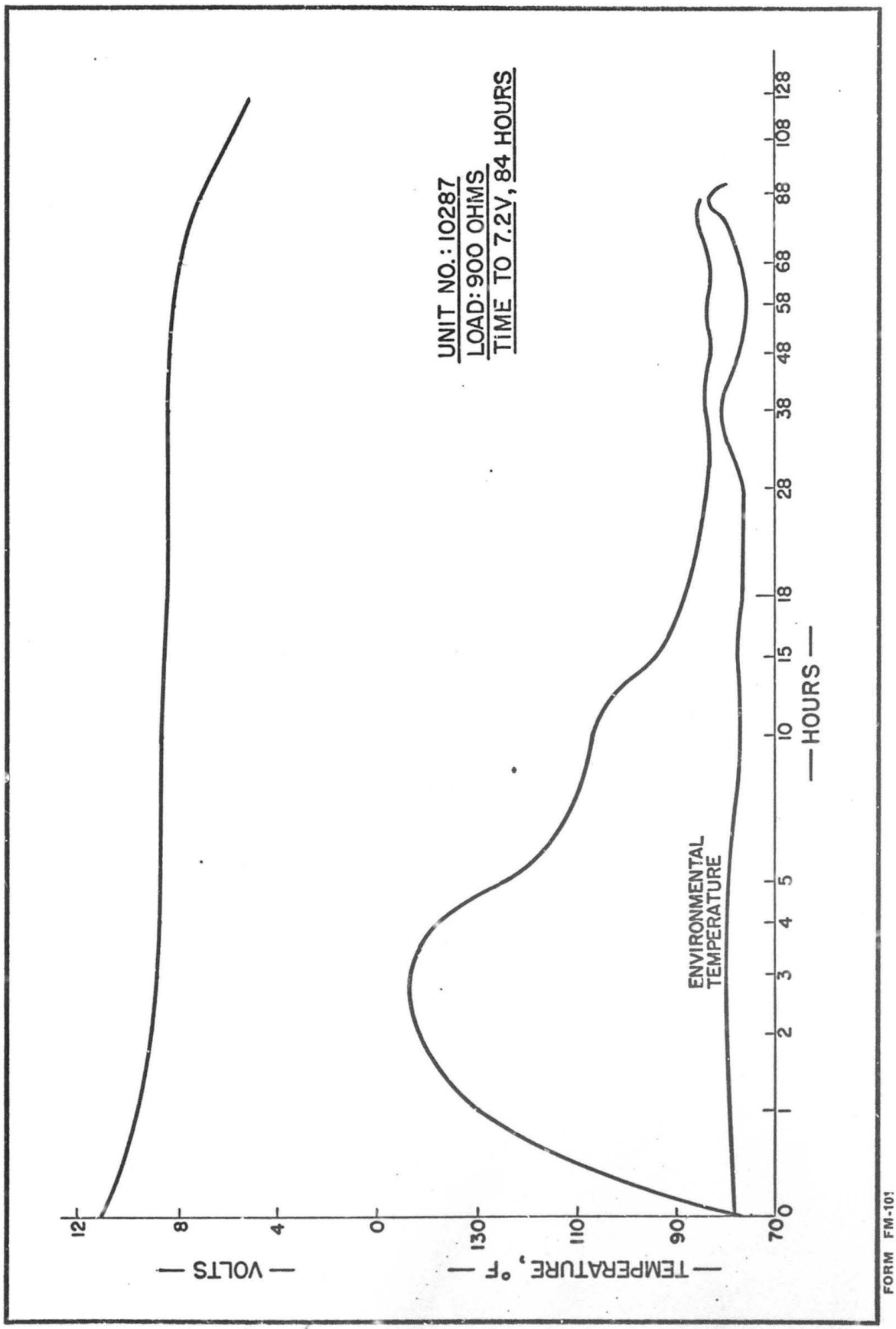
UNIT NO.: 10287
LOAD: 900 OHMS
TIME TO 7.2V, 84 HOURS
— VOLTS —
12
8
4
0
— TEMPERATURE, °F —
130
110
90
70
ENVIRONMENTAL TEMPERATURE
0
1
2
3
4
5
10
15
18
28
38
48
58
68
88
108
128
— HOURS —
FORM FM-101

FIGURE VI

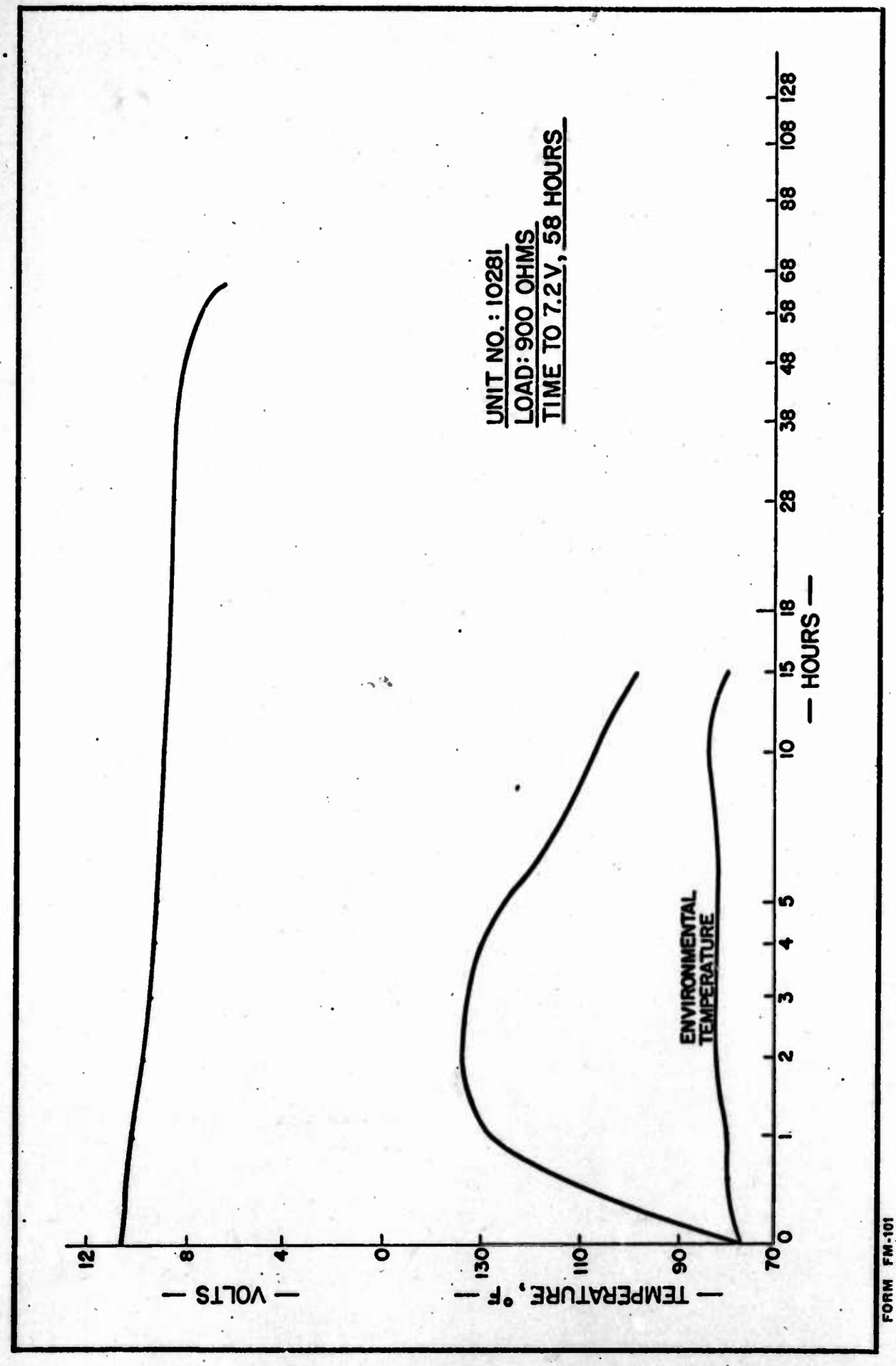
UNIT NO.: 10281
LOAD: 900 OHMS
TIME TO 7.2 V, 58 HOURS
— VOLTS —
12
8
4
0
— TEMPERATURE, °F —
130
110
90
70
ENVIRONMENTAL TEMPERATURE
0
1
2
3
4
5
10
15
18
28
38
48
58
68
88
108
128
— HOURS —
FORM FM-101

FIGURE VII

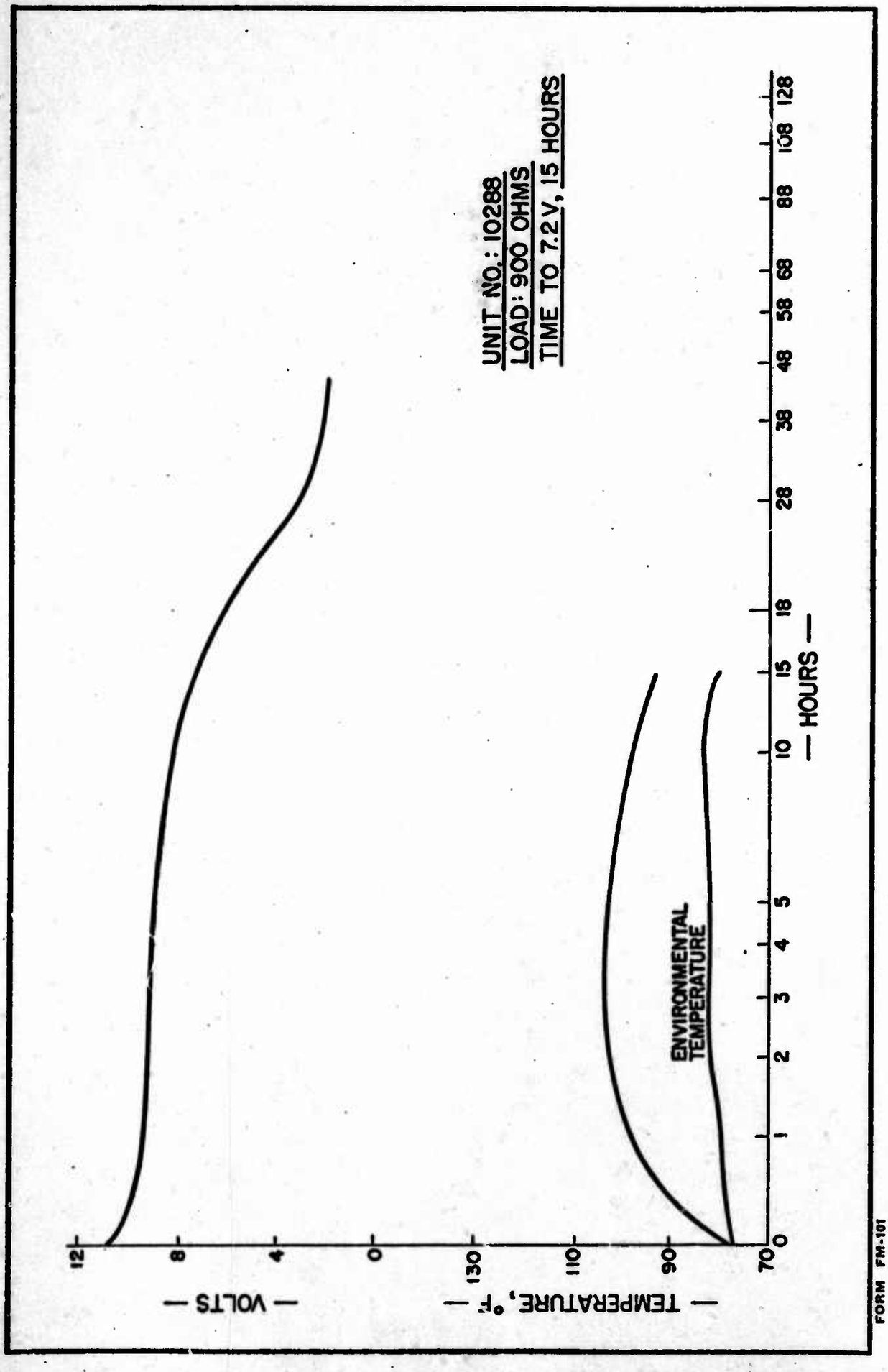
UNIT NO.: 10288
LOAD: 900 OHMS
TIME TO 7.2 V, 15 HOURS
— VOLTS —
12
8
4
0
— TEMPERATURE, °F —
130
110
90
70
ENVIRONMENTAL TEMPERATURE
0
1
2
3
4
5
10
15
18
28
38
48
58
68
88
108
128
— HOURS —
FORM FM-101

FIGURE VIII

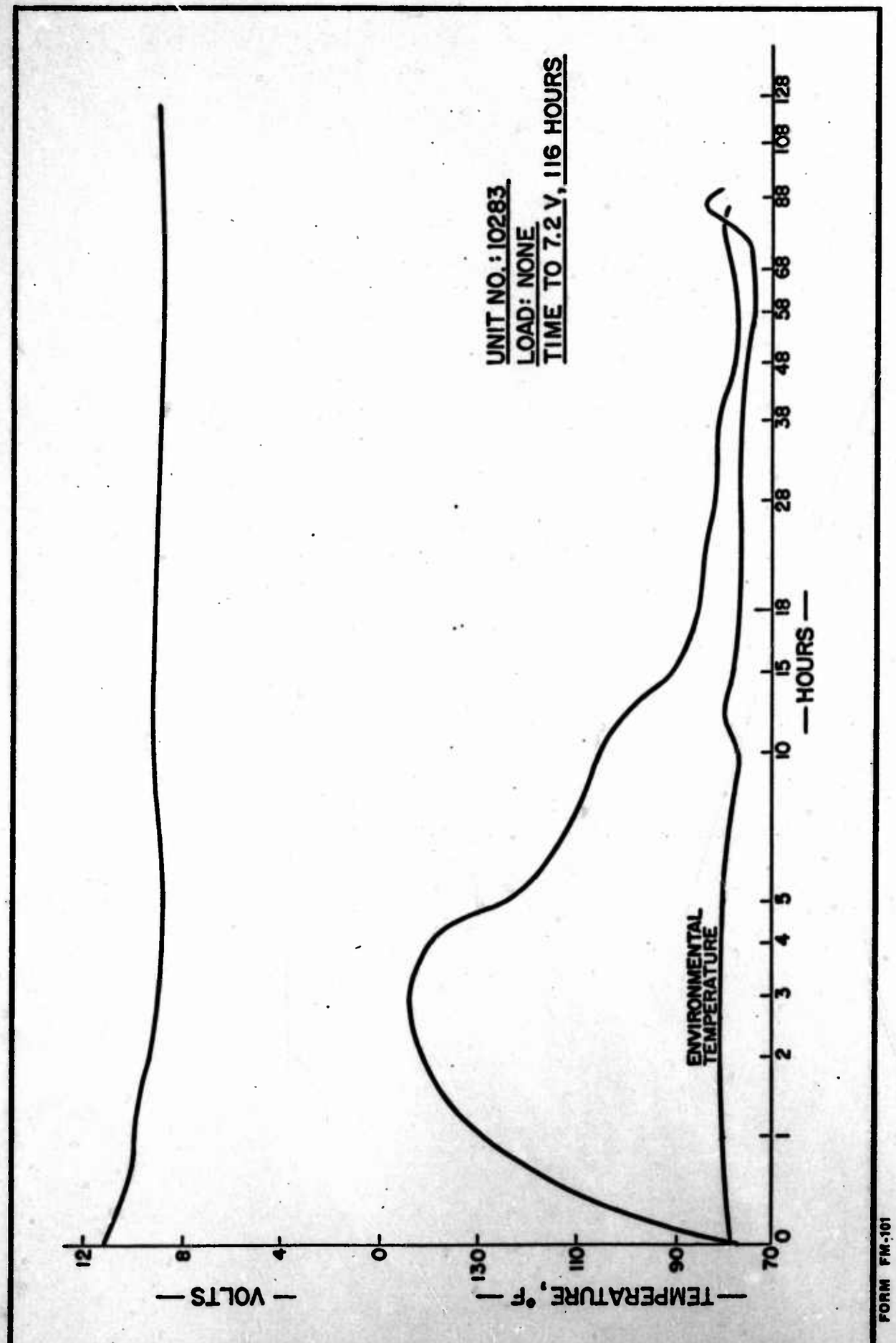
UNIT NO.: 10283
LOAD: NONE
TIME TO 7.2 V, 116 HOURS
— VOLTS —
12
8
4
0
— TEMPERATURE, °F —
130
110
90
70
ENVIRONMENTAL TEMPERATURE
0
1
2
3
4
5
10
15
18
28
38
48
58
68
88
108
128
— HOURS —
FORM FM-101

FIGURE IX

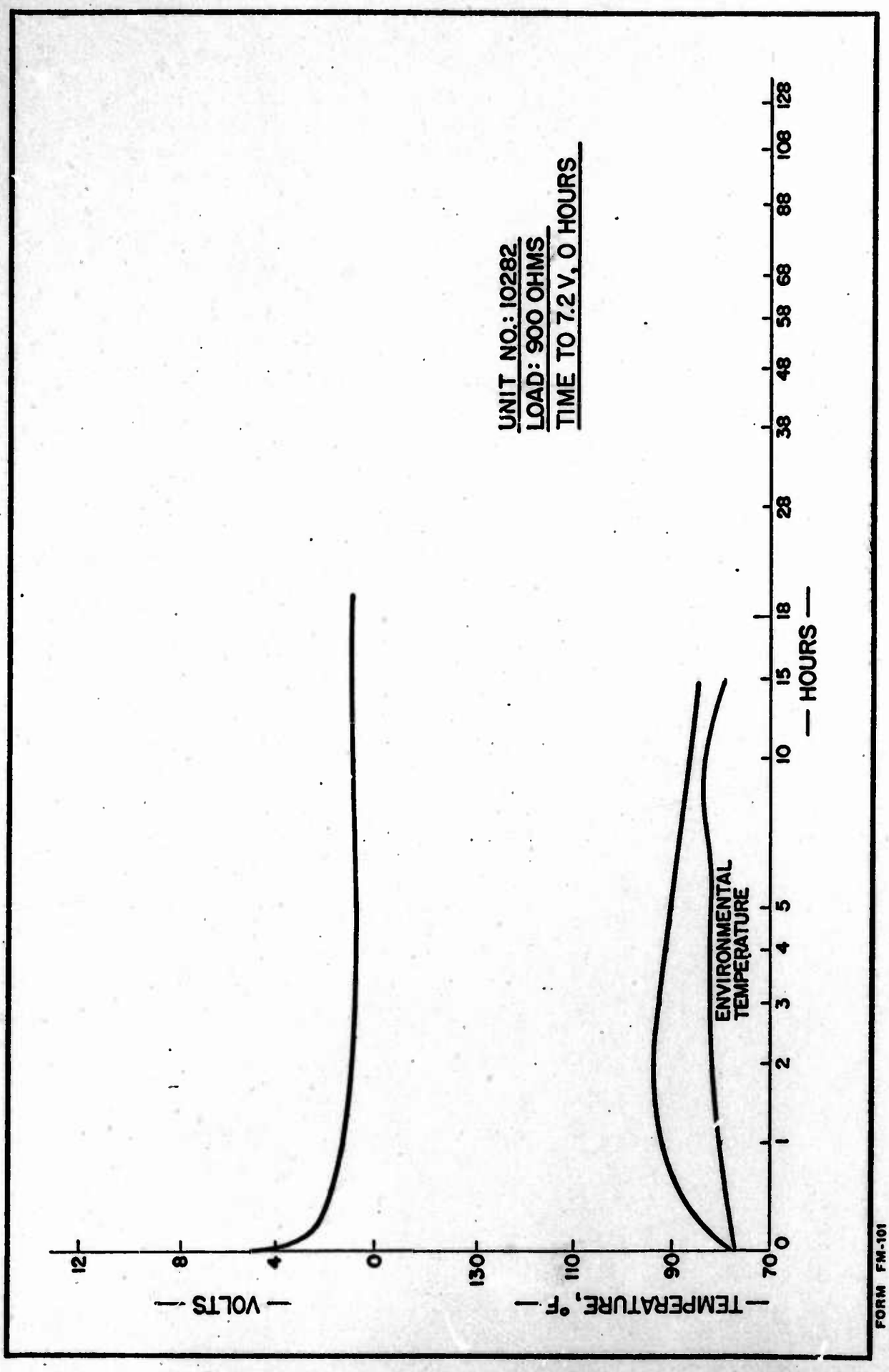
UNIT NO.: 10282
LOAD: 900 OHMS
TIME TO 7.2 V, 0 HOURS
— VOLTS —
12
8
4
0
— TEMPERATURE, °F —
130
110
90
70
ENVIRONMENTAL TEMPERATURE
0
1
2
3
4
5
10
15
18
28
38
48
58
68
88
108
128
— HOURS —
FORM FM-101

FIGURE X

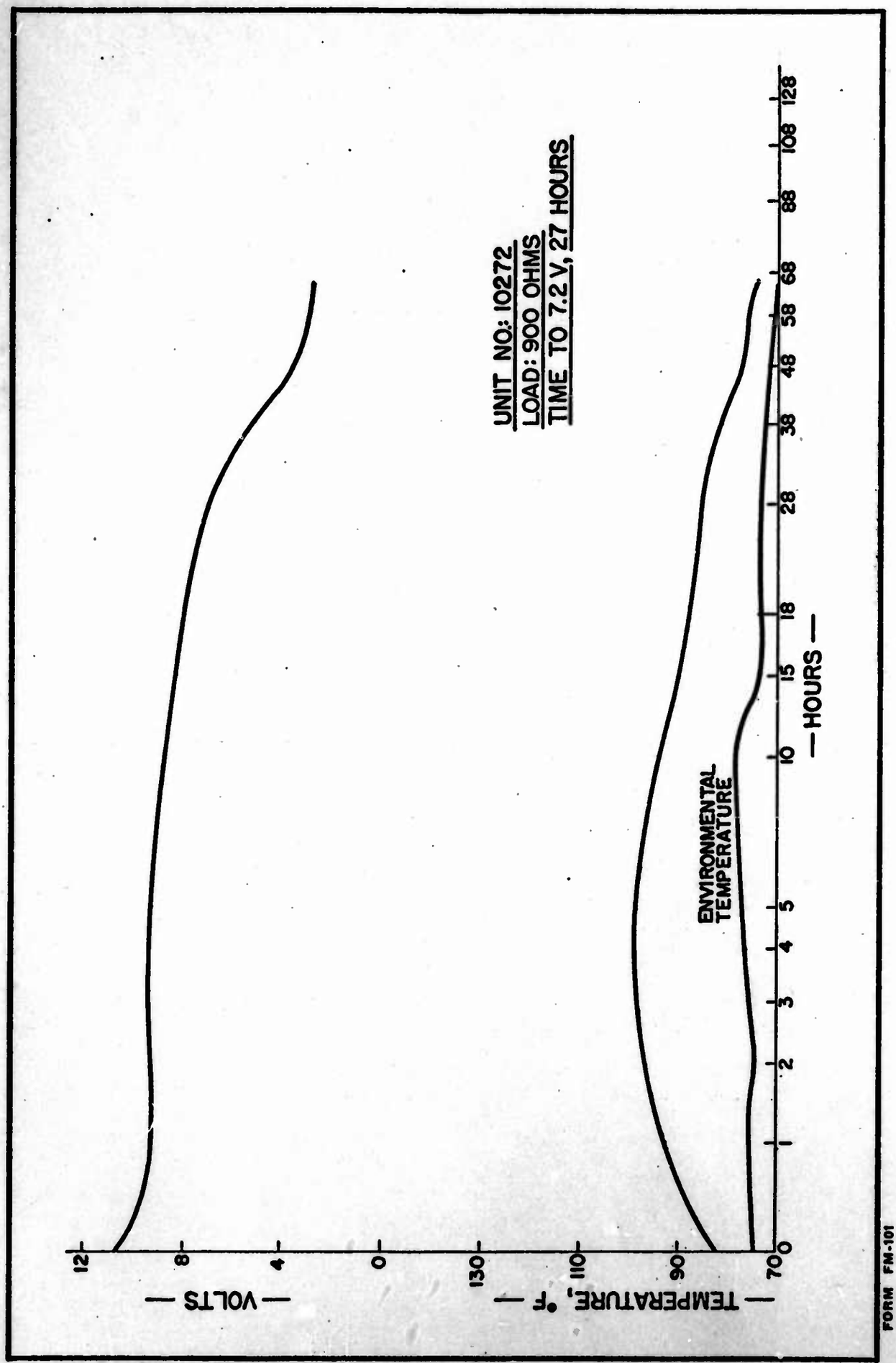
UNIT NO: 10272
LOAD: 900 OHMS
TIME TO 7.2 V, 27 HOURS
— VOLTS —
12
8
4
0
— TEMPERATURE, °F —
130
110
90
70
ENVIRONMENTAL TEMPERATURE
0
1
2
3
4
5
10
15
18
28
38
48
58
68
88
108
128
— HOURS —
FORM FM-101

FIGURE XI

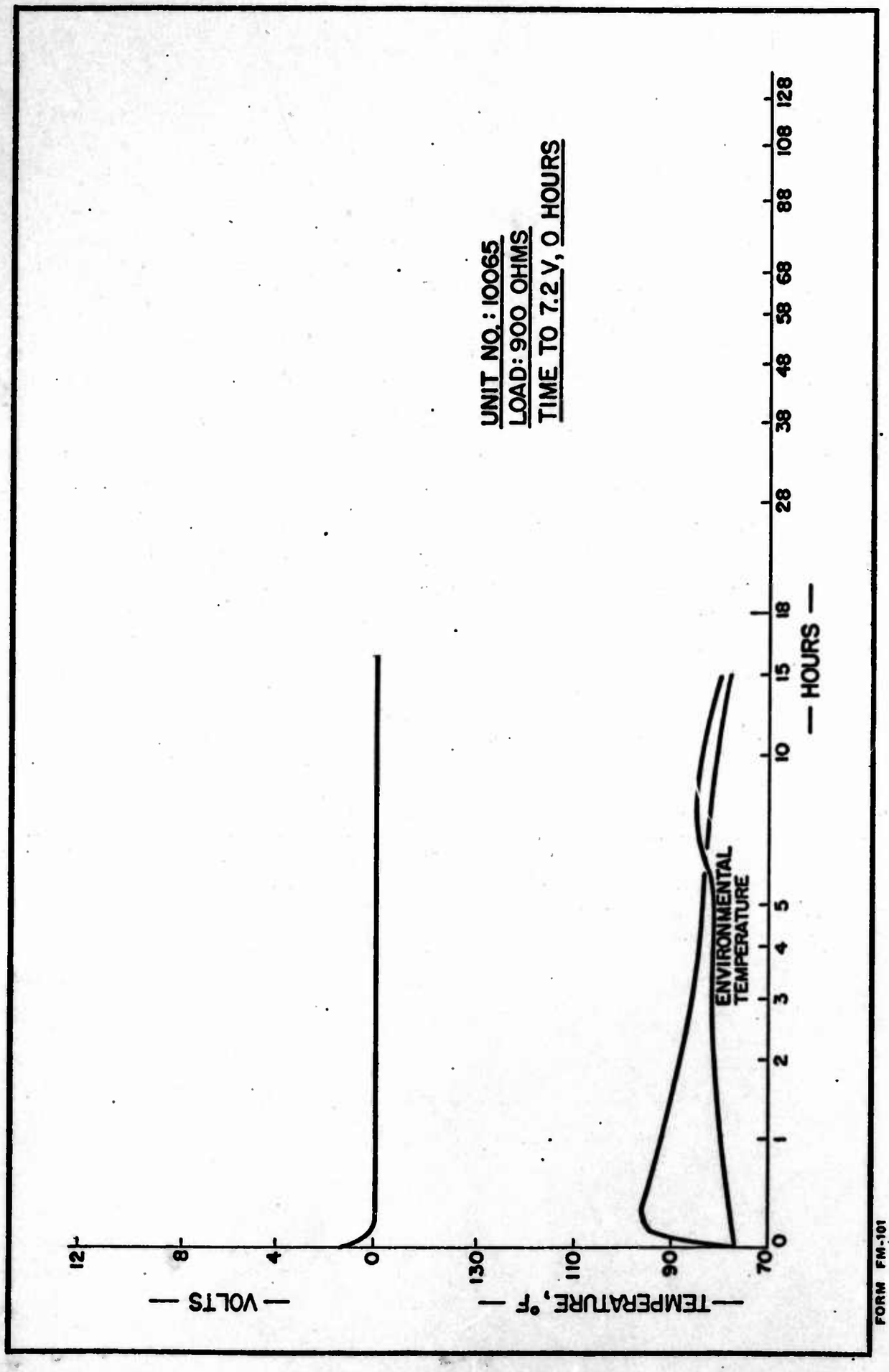
UNIT NO.: 10065
LOAD: 900 OHMS
TIME TO 7.2 V, 0 HOURS
— VOLTS —
12
8
4
0
— TEMPERATURE, °F —
130
110
90
70
ENVIRONMENTAL TEMPERATURE
0
1
2
3
4
5
10
15
18
28
38
48
58
68
88
108
128
— HOURS —
FORM FM-101

FIGURE XII

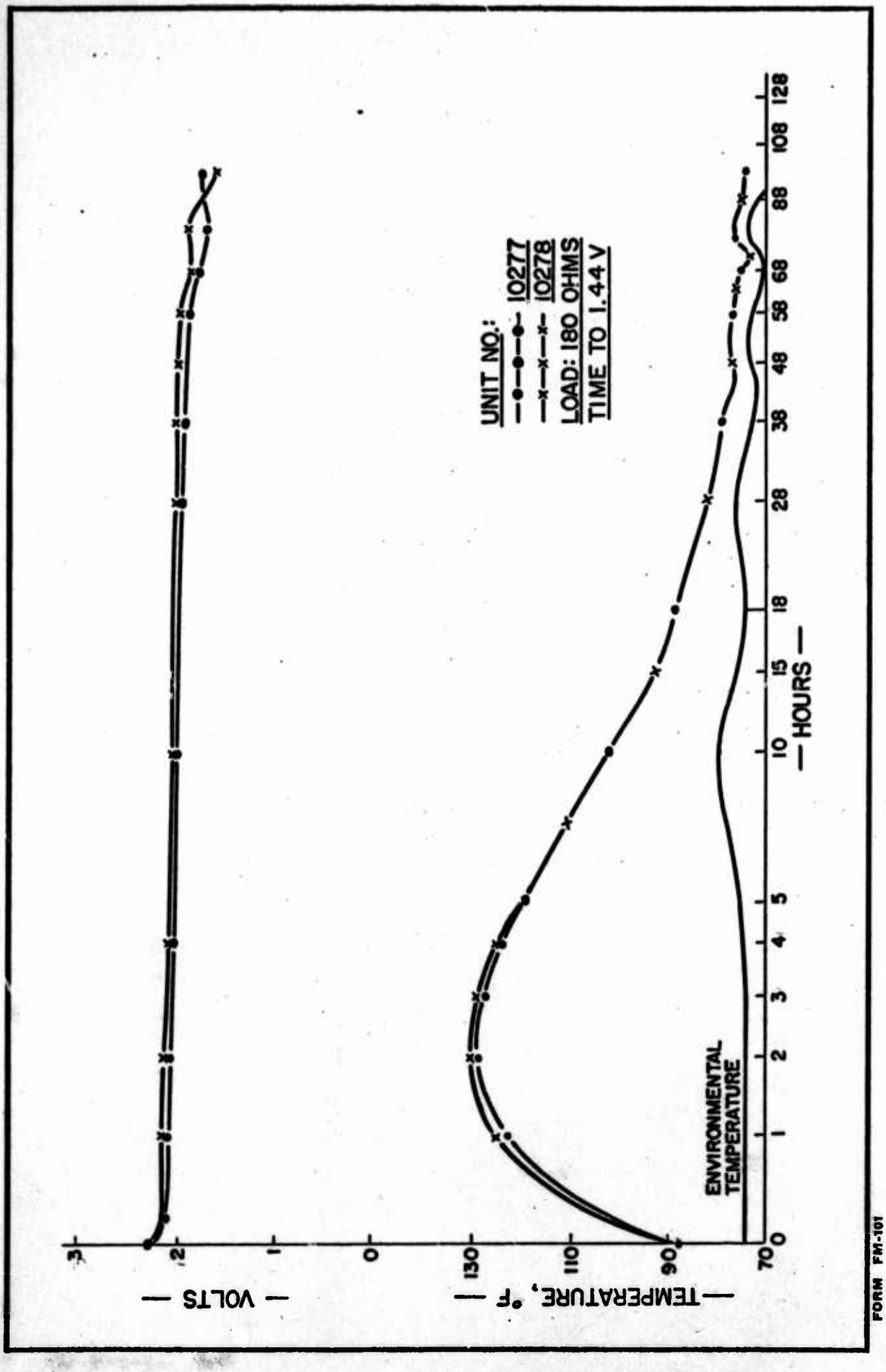
UNIT NO.:
10277
10278
LOAD: 180 OHMS
TIME TO 1.44 V
ENVIRONMENTAL TEMPERATURE
— VOLTS —
— TEMPERATURE, °F —
— HOURS —
FORM FM-101

FIGURE XIII